Available online at www.sciencedirect.com

ScienceDirect

Nuclear Physics B 945 (2019) 114673

NUCLEAR PHYSICS B

www.elsevier.com/locate/nuclphysb

Knots, links, anyons and statistical mechanics of entangled polymer rings

Franco Ferrari [a], Jarosław Paturej [a,b,*], Marcin Piątek [a,c], Yani Zhao [d]

[a] *Faculty of Mathematics and Physics, University of Szczecin, Wielkopolska 15, 70–451 Szczecin, Poland*
[b] *Leibniz-Institut für Polymerforschung Dresden e.V., 01069 Dresden, Germany*
[c] *Bogoliubov Laboratory of Theoretical Physics, Joint Institute for Nuclear Research, 141980 Dubna, Russia*
[d] *Max Planck Institute for Polymer Research, Ackermannweg 10, 55128 Mainz, Germany*

Received 7 February 2019; accepted 6 June 2019
Available online 7 June 2019
Editor: Hubert Saleur

Abstract

The field theory approach to the statistical mechanics of a system of N polymer rings linked together is extended to the case of links whose paths in space are characterized by a fixed number $2s$ of maxima and minima. Such kind of links are called $2s$-plats and appear for instance in the DNA of living organisms or in the wordlines of quasiparticles associated with vortices nucleated in a quasi-two-dimensional superfluid. The path integral theory describing the statistical mechanics of polymers subjected to topological constraints is mapped here into a field theory of quasiparticles (anyons). In the particular case of $s = 2$, it is shown that this field theory admits vortex solutions with special self-dual points in which the interactions between the vortices vanish identically. The topological states of the link are distinguished using two topological invariants, namely the Gauss linking number and the so-called bridge number which is related to s. The Gauss linking number is a topological invariant that is relatively weak in distinguishing the different topological configurations of a general link. The addition of topological constraints based on the bridge number allows to get a glimpse into the non-abelian world of quasiparticles, which is relevant for important applications like topological quantum computing and high-T_C superconductivity. At the end an useful connection with the cosh-Gordon equation is shown in the case $s = 2$.

* Corresponding author.
E-mail addresses: franco@feynman.fiz.univ.szczecin.pl (F. Ferrari), piatek@fermi.fiz.univ.szczecin.pl (M. Piątek).

https://doi.org/10.1016/j.nuclphysb.2019.114673

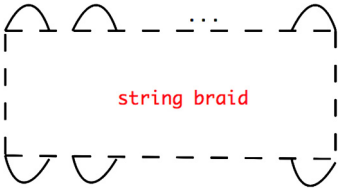

Fig. 1. A plat obtained by joining together the ends of a set of braided strings both at the top and at the bottom. The ends of the strings that are nearest to each other are connected together in pairs with the help of arcs. In the figure only the arcs are visible, while the braided stings are inside the dashed rectangular area.

1. Introduction

Knots and links are a fascinating subject and are researched in connection with several concrete applications both in physics and biology [1–32]. A beautiful review from a theoretical physicist point of view about knot theory and polymers can be found in Ref. [33], Chapter 16. In this paper we study the statistical mechanics of a system of an arbitrary number of entangled polymer rings. Mathematically, two or more entangled polymers form what is called a link. Single polymer rings form instead knots. We will restrict ourselves to links in the configurations of $2s$-plats. Roughly speaking, $2s$-plats are knots or links obtained by braiding together a set of $2s$ strings and connecting their ends pairwise [34]. More precisely, a $2s$-plat is obtained from a $2s$-braid $\beta = B_{2s}$ by closing it with $2s$ simple arcs [34,35]. The way in which a general braid can be closed is not unique. In the case of plats, the $2s$ strings forming the braid are closed by arcs in the way illustrated in Fig. 1. Clearly, after the plat-type closure shown in Fig. 1, it turns out that $2s$-plats consist of closed paths characterized by s maxima and s minima. The result of the operation of plat closure of Fig. 1 is a knot (or link) diagram on the two dimensional plane, with a system of overpasses and underpasses simulating the three dimensional structure of the original knot (or link), see Figs. 2 and 3.[1] Overpasses and underpasses meet at points that are called crossings.

Besides plats, the other mostly used convention for braid closure is called strand closure [36]. While in a plat closure the number of strings is always even ($2s$), in the case of strand closures this number can be both even or odd. Plats are very general constructions in knot theory. Indeed, it has been shown that any unoriented knot or link in S^3 can be realized as a $2s$-plat [35,37]. This is due to a theorem of Alexander [38] stating that all knots and links admit a representation as closed braids [38,39]. It turns out that the number $2s$ of strings in a braid that should be used in order to represent a given knot or link as a plat is bound from below. For instance, an unknotted ring, also called the unknot and denoted according to the Rolfsen table 0_1, is the only knot type that can be constructed from the closure of two strings. The trefoil knot 3_1 requires instead a minimal number of strings equal to four. In a general link composed by N unknots, it is easy to realize that the smallest value of s is reached when the unknotted rings have only a maximum and one minimum, i.e. $s_{min} = 2N$. The least number of strings corresponding to a plat closure representation of a knot or link is equal to twice the so-called bridge number, a topological

[1] Technically, an overpass is defined as a subarc in the diagram of a knot whose path is not interrupted at least at one crossing. Going along the subarc in both directions allowed, we will encounter sooner or later a crossing in which the path is interrupted. A maximal overpass is the longest overpass that it is possible to obtain without breaking the lines of the subarc. For instance, the trefoil knot of Fig. 2 contains two maximal overpasses.

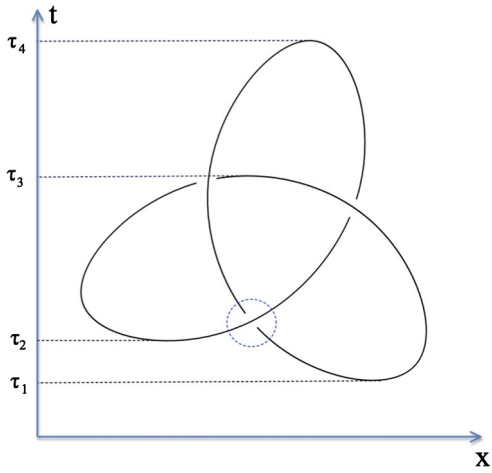

Fig. 2. Representation of a trefoil knot in terms of a two-dimensional diagram. The τ_i's, $i = 1, \ldots, 4$, denote the heights of the points of minima and maxima.

Fig. 3. The figure shows one of the crossings which are present in the diagram of the trefoil knot of Fig. 2.

invariant that denotes the minimal number of maximal overpasses necessary to represent a given knot [40].

A physical realization of $2s$-plats in the case of polymers could be a set of ring-shaped polymers in which some of the monomers are grafted to two membranes or surfaces located at two different heights. If the chains are rigid enough, the formation of turn points, a fact that could change the number of maxima and minima of the plat obtained in this way, can be eliminated. In nature $2s$-plats occur for example in the DNA of living organisms [13,29,30,41]. Indeed, it is believed that most knots and links formed by DNA are in the class of 4-plats [13]. This fact may depend on the rigidity of DNA, that prevents the formation of further bendings necessary to build six or higher order plats in the short strands of DNA arising after the action of the so-called topoisomerases, the enzymes discussed in [13]. The relevance of plats in biology and biochemistry have inspired the research of Ref. [42], in which 4-plats have been studied with the methods of statistical mechanics and field theory. In particular, in [42] it has been established an analogy between polymeric 4-plats and anyons, showing in this way the tight relations between two-component systems of quasiparticles and the theory of polymer knots and links. After the publication of [42], interesting applications of two-component anyon systems in topological quantum computing have been proposed [43–45]. These applications are corroborated by the results of experiments concerning the detection of anyons obeying a nonabelian statistics, see for example [46]. While these results have appeared in 2005 and are still under debate [45,47], other systems in which non-abelian anyon statistics could be present have been discussed [48,49]. A more recent extensive report on topological quantum computing with non-abelian anyons may be found in [50]. Physical systems that have been proposed in order to implement topological quantum computations are quasiparticles in the form of vortices nucleated in a quasi two-dimensional superfluid. Concrete experimental realizations of such systems are mentioned in [50].

Motivated by these advances, we study here the general case of $2s$-plats in which N polymer rings are entangled together to form a link. Let us recall that two links are topologically equivalent if they can be transformed one into the other by means of continuous deformations. Here the topology of the link will be determined using two topological invariants, namely the Gauss linking number (GLN) and the bridge number discussed above. The simultaneous application of the Gauss linking number and of the bridge number goes beyond the limitations of the abelian anyon models that are obtained using only the GLN and allows to get a glimpse into the non-abelian world that is relevant in topological quantum computing and high-T_C superconductivity.

The first result in this work is to derive a field theoretical model describing the statistical mechanics of a link composed by N rings concatenated together to form the configuration of a $2s$-plat. The points of maxima and minima of the plat are kept fixed. To mimic the situation in which these points correspond to polymer bonds that are grafted on membranes, the heights of these points in the z-direction are taken to be arbitrary. Links of this type have already been discussed in Ref. [51], where they have been called deformed plats to distinguish them from the mathematical plats, in which maxima and minima are distributed respectively at the two heights z_{max} and z_{min}. Let us notice that the analogy between polymers and quasiparticles requires that the maxima are all at the height z_{max} and the minima at the height z_{min}. The configuration of a $2s$-plat allows to split the link into $2s$-directed paths. In principle the partition function of $2s$-directed chains could be formulated using the path integral formalism and mapped into a field theory using standard techniques explained for instance in [33]. This strategy is however complicated by the topological constraints based on the Gauss linking number. The approach of Ref. [52], that uses a set of BF-fields to impose conditions on the Gauss linking numbers of N topologically entangled rings, cannot be applied to the present system. The reason is that such approach is valid for a general link and does not take into account the further constraints that are necessary to keep the desired $2s$-plat configuration. The problem of implementing the GLN constraints has been solved in the case of 4-plats in Ref. [42]. Here the results of [42] are generalized to the more complicated situation in which there are $2s$-paths, each of them having the possibility of winding up around another. The topological field theories implementing the conditions on the GLN are quantized in the Coulomb gauge. This gauge has the advantage of making the connection between polymers and quasiparticles particularly evident. The details of our method, that could not be provided in a short letter like [42], are explained in details.

After the passage to the second quantized fields is realized, a model describing a gas of quasiparticles is obtained. All the nonlocalities and strong nonlinearities due to the topological constraints that characterize the original first quantized theory of polymers disappear in the field theoretical formulation. The polymer paths become wordlines describing the motion of the quasiparticles, while the densities of monomers may be regarded as quasiparticle densities of a multi-layered anyon gas. The evolution of the positions of the quasiparticles is followed from the initial time $\tau_0 = z_{min}$ to the final time $\tau_1 = z_{max}$, where the time t flows along the z-axis. As already mentioned, systems of this type, in which the worldlines of quasiparticles are braided together, are relevant in quantum computing, as they have been proposed as logic gates in prototypes of topological quantum computers.

In the context of quantum computing, a remarkable feature of the field theoretical model derived here starting from the partition function of polymer links in the configuration of a $2s$-plat is that it admits self-dual points. The action of the quasiparticles can be in fact minimized by self-dual solutions of the classical equations of motion. From the polymer point of view, this self-duality has a simple physical explanation. Due to the topological constraints, the lines of knots and links can attract or repel themselves. For instance, unknotted rings are known to repel

also in the absence of excluded volume interactions. On the contrary, when the rings are linked together, their lines get closer, a fact that has been experimentally verified by measuring the average distance between the centers of mass of two DNA rings linked together and can be predicted using field theoretical methods [53]. The more complex is the topological configuration of the link, the smaller is the distance [53]. In the particular case of a $4s$-plat, it was already shown in [42] that, after a Bogomol'nyi transformation, it is possible to single out in the two-body forces of entropic origin that are related to the topological constraints contributions that, apart from proportionality constants, are exactly of the form of the excluded volume forces, but can be both attractive and repulsive. For certain values of the parameters of the model, namely the Kuhn lengths and the total lengths of the $2s$ open chains composing the plat, it turns out that the attractive and repulsive components of these forces disappear giving rise to the self-dual point. With respect to [42] we prove here always in the case of a 4-plat that the vortex solutions may be explicitly constructed after solving a cosh-Gordon equation. Let us finally recall that polymer $2s$-plats can be realized in the laboratory with present technologies [54]. Our results show that at least in 4-plats there are self-dual conformations that are particularly stable. The effects of the presence of these conformations could be experimentally measurable.

Apart from the existence of self-dual solutions, the field theoretical model developed in this work has also phenomenological consequences that are relevant for the statistical mechanics of polymers. First of all, its Lagrangian contains a local, analytic and nonperturbative expression of the interaction terms which describe the topological forces acting on the monomers. These forces, which appear due to the constraints that limit the topological configuration of the $2s$-plat, have two-body and three-body components. The two-body interactions have already been studied with the help of the method of the effective potential in [55]. It has been found there that the monomers of two heavily entangled polymer rings attract themselves due to the topological constraints counterfeiting the excluded volume interactions typical of polymers in a good solution. What is unespected is the presence of three-body interactions in a polymer system subjected to topological constraints imposed with the help of the Gauss linking number. The appearance of three-body forces of topological origin is surprising because the Gauss linking number is able to take into account only the topological relations between pairs of knotted polymer rings. For this reason, one could expect that this type of constraints should be rather associated with interactions between pairs of monomers belonging to two different chains. Indeed, the explicit expression of the Gauss linking number can be interpreted as a (nonlocal) two-body potential related to forces acting on the bonds located on two different polymers. Three-body forces have been proved to vanish in the case of links with two polymers only, see Ref. [55]. However, we show here that there are processes in which three-body forces are relevant if the number of loops involved in the link is equal to three or higher.

This paper is organized as follows. First, we split the lines of the N polymer rings forming a $2s$-plat into a set of $2s$ open chains. The splitting procedure and the definition of a suitable "time" variable that parametrizes the $2s$ chains is carefully described in Section 2. In Section 3 it is shown how it is possible to implement and simplify in the partition function of the $2s$-plat the constraints that fix the possible topological configurations in which the system of polymer rings linked together can be found. The constraints are imposed using the Gauss linking number. The treatment follows the method already established in Ref. [56], but its generalization to the case in which the link is splitted into a set of $2s$ open chains parametrized by the special "time" coordinate instead of the usual arc-lengths is new. To eliminate the nonlinearities and nonlocalities introduced by the topological constraints, which necessarily have memory since they must remember the global geometry of the ring in space, we use a set of abelian BF-fields. These

fields generate electromagnetic type interactions acting on the monomers and create in this way the necessary "reaction" forces that forbid the system to escape the topological constraints. Next, the BF-field theory is quantized in the non-covariant Coulomb gauge. This gauge leads to several simplifications and is very convenient in order to establish the analogy with anyon systems. How the "covariance" of the theory is recovered is shown in Appendix C in the particular case of a 4-plat. This example is very helpful to interpret the meaning of the Gauss linking number in the Coulomb gauge, which is otherwise apparently more related to the winding number of open polymers than to the Gauss linking number itself. In Section 4 the passage from first quantized polymer chains to second quantized fields is performed. The case of general interactions between the monomers is considered. After the second quantization procedure and the introduction of replica complex scalar fields, the densities of monomers of the original polymer rings can be regarded as the densities of a system of multilayered gas of quasiparticles. The topological BF-fields are eliminated by integrating them out from the partition function. In this way quartic and sestic interactions terms appear in the action, corresponding to two and three body interactions respectively. In Section 5 some phenomenological consequences on the statistical mechanics of the $2s$-plat coming from the field theoretical model obtained in Section 4 are presented. In Section 6 we limit ourselves to 4-plats, switching off the non-topological interactions. In this particular case, studied in Ref. [42], it is known that the Hamiltonian of the 4-plat is minimized by self-dual solutions. Here the classical equations of motion are reduced to a cosh-Gordon equation. It is shown how the explicit expression of the classical configurations minimizing the Hamiltonian of the 4-plat can be constructed out of the solution of this cosh-Gordon equation. Finally, our conclusions are drawn in Section 7.

2. Polymers as $2s$-plats

Let's consider N closed loops $\Gamma_1, \ldots, \Gamma_N$ of lengths $L_1, \ldots, L_N$ respectively in a three-dimensional space with coordinates $(\boldsymbol{r}, z)$. The vector $\boldsymbol{r} = (x, y)$ spans the two dimensional space $\mathbb{R}^2$. The N loops will be labeled using as indices the first letters of the latin alphabet: $a, b, c, \ldots = 1, \ldots, N$. We will assume and ensure by means of suitable constraints that $\Gamma_1, \ldots, \Gamma_N$ form a $2s$-plat. The heights of the points belonging to a $2s$-plat will be measured here using the z coordinate. As it will be shown in Subsection 3.1, the choice of a special direction is not decreasing the degree of generality. Similar setups have been already studied in the literature, see for instance [51,57]. The trefoil diagram in Fig. 2 provides an example of a knot in the 4-plat configuration characterized by two points of minima and two maxima. Another example of 4-plats, this time a link composed by two concatenated rings, is given in Fig. 4.

In the following we will deal with the deformed $2s$-plats studied in Refs. [51,57], in which the maxima and minima are at different heights. s is kept constant as a requirement and the locations of the points of maxima and minima are fixed, i.e. they are not allowed to fluctuate. Summing over all possible values of s, i.e. over all integers $s \geq s_{min}$ and integrating over all allowed positions of the maxima and minima for each value of s, the partition function of N polymer rings without further constraints apart from being linked together should be recovered. To perform such sum over s and the integration over the locations of the maxima and minima is however very complicated and it is not necessary for the aims of the present work. To establish the desired analogy between systems of linked polymer rings and quasiparticles, in fact, we need actually not only that the maxima and minima are fixed points, but also that the maxima and minima are respectively at the same heights z_{max} and z_{min}.

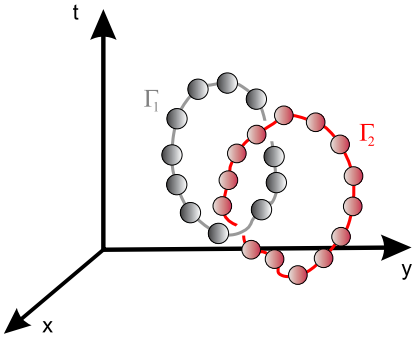

Fig. 4. A link formed by two polymer rings Γ_1 and Γ_2.

Let us denote with the symbols τ_{a,I_a}, $I_a = 0, \ldots, 2s_a - 1$, the heights of the maxima and minima of each loop Γ_a, for $a = 1, \ldots, N$. Of course, it should be that

$$\sum_{a=1}^{N} s_a = s. \tag{1}$$

We choose $\tau_{a,0}$ to be the height of the point of absolute minimum of the loop Γ_a. Starting from this point, we select the orientation of Γ_a in such a way that, proceeding along this loop according to that orientation, we will encounter in the order a point of maximum at the height $\tau_{a,1}$, the next point of minimum at the height $\tau_{a,2}$ and so on. We denote with $2s_a$ the total number of maxima and minima of the loop Γ_a. The heights of these points will be: $\tau_{a,0}, \tau_{a,1}, \tau_{a,2}, \ldots, \tau_{a,2s_a-1}$. Clearly, the point with height $\tau_{a,2s_a-1}$ is a point of maximum. To simplify the notations, it is convenient to add the height

$$\tau_{a,2s_a} \equiv \tau_{a,0}. \tag{2}$$

The introduction of two symbols $\tau_{a,0}$ and $\tau_{a,2s_a}$ for the height of the same point, that of the absolute minimum of the loop Γ_a, will be useful in the future in order to write formulas in a more compact form. In the following, the loops $\Gamma_1, \ldots, \Gamma_N$ will be decomposed into a set of directed paths Γ_{a,I_a}, $a = 1, \ldots, N$ and $I_a = 1, \ldots, 2s_a$, whose ends are made to coincide in such a way that they form the topological configuration of two linked rings. Due to the analogy of these paths with the trajectories of two-dimensional quasiparticles, they will be called hereafter "trajectories". An example of such trajectories when $s = 3$ and $N = 1$ is presented in Fig. 5. In the general case, the set of points belonging to Γ_{a,I_a} can be described by the formula:

$$\Gamma_{a,I_a} = \left\{ \boldsymbol{r}_{a,I_a}(t_{a,I_a}) \;\middle|\; \begin{array}{ll} a = 1, \ldots, N; & I_a = 1, \ldots, 2s_a \\ \left\{ \begin{array}{ll} \tau_{a,I_a-1} \le t_{a,I_a} \le \tau_{a,I_a} & I_a \text{ odd} \\ \tau_{a,I_a-1} \ge t_{a,I_a} \ge \tau_{a,I_a} & I_a \text{ even} \end{array} \right. \end{array} \right\} \tag{3}$$

where the additional boundary conditions:

$$\boldsymbol{r}_{a,I_a}(\tau_{a,I_a}) = \boldsymbol{r}_{a,I_a+1}(\tau_{a,I_a}) \qquad I_a = 1, \ldots, 2s_a - 1 \tag{4}$$

$$\boldsymbol{r}_{a,1}(\tau_{a,0}) = \boldsymbol{r}_{a,2s_a}(\tau_{a,0}) \tag{5}$$

are understood. These conditions are needed in order to connect together the trajectories Γ_{a,I_a} so that the loop Γ_a is reconstructed. The variables t_{a,I_a} defined in Eq. (3) are very convenient when considering curvilinear integrals around a loop Γ_a that is split into many trajectories Γ_{a,I_a}. The

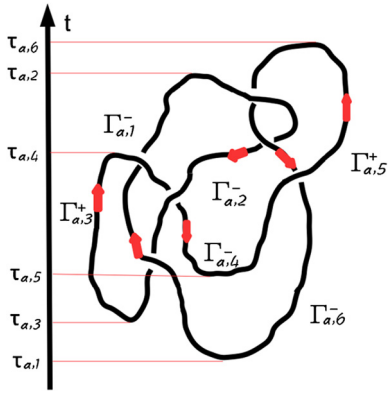

Fig. 5. Sectioning procedure for a $2s$-plat Γ_a with $s = 3$ into a set of directed paths Γ_{a,I_a} (see text for details).

technical details of how these variables have been introduced and an example of how they work in curvilinear integrals are presented in Appendix A.

3. Fixing the topological properties of a $2s$-plat: the case of the Gauss linking number

In the case of a $2s$-plat composed by N loops $\Gamma_1, \ldots, \Gamma_N$, it is possible to specify the winding number between any two trajectories Γ_{a,I_a} and Γ_{b,I_b} composing the plat. These winding numbers cannot change due to the thermal fluctuations, because the end points $(\boldsymbol{r}(\tau_{a,I_a-1}), \tau_{a,I_a-1})$ and $(\boldsymbol{r}(\tau_{a,I_a}), \tau_{a,I_a})$ of each trajectory Γ_{a,I_a} must be fixed in our construction. This fact can be used to constrain the $2s$-plat to stay in very complex topological configurations. In the following, however, we will not adopt this strategy. The topological configurations of the system will rather be imposed by applying the Gauss linking number.

3.1. The standard approach of imposing the constraints with the Gauss linking number

The Gauss linking number is a link invariant expressing the topological states of two closed trajectories linked together. Due to the fact that it can only be applied to pairs of loops, here we restrict ourselves for simplicity to the case of a $2s$-plat composed by only two loops Γ_1 and Γ_2. Note that each of these two loops is a plat too having s_a points of maxima and s_a points of minima with $a = 1, 2$. For consistency, it should be that $s = s_1 + s_2$. The Gaussian linking number is defined as follows

$$\chi(\Gamma_1, \Gamma_2) = \frac{1}{4\pi} \epsilon_{\mu\nu\rho} \oint_{\Gamma_1} d\tilde{x}_1^{\mu}(d_1) \oint_{\Gamma_2} d\tilde{x}_2^{\nu}(d_2) \frac{(\tilde{x}_1(d_1) - \tilde{x}_2(d_2))^{\rho}}{|\tilde{x}_1(d_1) - \tilde{x}_2(d_2)|^3} \tag{6}$$

where the $\tilde{x}_a^{\mu}(d_a)$'s and the arc-lengths d_a's, $a = 1, 2$ have been defined in Appendix A, after Eq. (133). The Gauss linking number has the advantage that it is easy to be implemented in a field theory because it is related to an abelian BF-model [56]. The price of this simplicity is that the set of transformations that do not change the value of the GLN is larger than that of the continuous deformations and contains also transformations that break the lines of the polymers. As a consequence, many inequivalent topological configurations characterized by the same value of the Gauss linking number are allowed. For example, the unlink and the Whitehead link are

clearly topologically inequivalent, but they are equivalent according to the Gauss linking number, because this topological invariant is equal to zero in both cases. For this reason, the GLN is a weak topological invariant. However, it is easy to realize that the additional requirement that the conformations of a link can change only within the class of $2s$-plats with a fixed number $2s$ of maxima and minima removes in part the limitations of the GLN. If we start from an unlink in the form of a 4-plat, for instance, it is not possible to obtain a Whitehead link acting on the unlink with transformations that keep fixed both the GLN and the number of maxima and minima. Indeed, the minimum allowed number of maxima and minima of the Whitehead link is six, so that this link cannot be reduced to a 4-plat. Vice-versa, it will not be possible to obtain a 4-plat unlink acting on a 6-plat Whitehead link. For the sake of generality, in the present work we will allow for arbitrary values of s. The treatment of the constraints in the proposed field theoretical model can be made mathematically rigorous by imposing additionally that s coincides with the least possible value s_{min} for a link of a given type, i.e. with its bridge number. As already explained before, in a link composed by N unknots $s_{min} = 2N$. If we would like to select a link consisting of N trefoil knots, for example, it turns out that $s_{min} = 4N$. Of course, this way of specifying the topology of the knots composing the link is very rough. Only the condition $s_{min} = 2N$ determines uniquely a set of N unknotted rings. In all the other case different mixtures of knots of different topological types are allowed.

Having in mind the analogy with systems of quasiparticles that will be established here, the $2s$ chains of the open polymers could also be viewed as the trajectories of $2s$ particles moving on a two-dimensional space, while the time t flows along the z-direction. This is very important for the realization of the mapping between polymers and quasi-particles that is one of the main results of the present paper. We would like to stress that the choice of a particular direction in space does not spoil the generality of our treatment. Indeed, the only effect of a rotation could be that the number of maxima and minima of the plat could change to a new value s' such that $s' \neq s$. This fact does not represent a problem, because our calculations are valid for any value of s. On the other side, the value of the Gauss linking number does not depend on the way in which the system is rotated. Following the original implementation of the field theoretical formulation of the statistical mechanics of polymer links in which the topological constraints are imposed with the help of the GLN, see Ref. [56], this link invariant can be associated to a BF-model. In the presence of a preferred direction non-covariant gauge fixings are the most convenient. In the case of static knots — i.e. knots that not subjected to thermal fluctuations —, the light-cone gauge has been applied, see for instance Refs. [51] and [57]. In this work we prefer to use the Coulomb gauge, whose consistency in the frame of the so-called Chern-Simons field theories has been rigorously tested [58]. As it will be shown in Appendix C, the GLN is unaffected by our gauge choice.

Coming back to Eq. (6), the trajectories of the two loops Γ_1 and Γ_2 will be topologically constrained by the GLN condition

$$m_{12} = \chi(\Gamma_1, \Gamma_2) \tag{7}$$

m_{12} being a given integer and $\chi(\Gamma_1, \Gamma_2)$ is defined in (6). The constraint (7) is imposed by inserting the Dirac delta function $\delta(m_{12} - \chi(\Gamma_1, \Gamma_2))$ in the partition function of the $2s$-plat, where the statistical sum over all conformations of Γ_1 and Γ_2 is performed. Of course, the analytical treatment of such a delta function in a path integral is difficult. Some simplification is obtained by passing to the Fourier representation

$$\delta(m_{12}-\chi(\Gamma_1,\Gamma_2))=\int\limits_{-\infty}^{+\infty}\frac{d\lambda_{12}}{\sqrt{2\pi}}\,\mathrm{e}^{-i\lambda_{12}(m_{12}-\chi(\Gamma_1,\Gamma_2))}. \tag{8}$$

Even in the Fourier representation, the difficulty of having to deal with the Gauss linking number in the exponent appearing in the right hand side of Eq. (8) remains. Formally, this link invariant introduces a term that resembles the potential of a two-body interaction which is both nonlocal and nonpolynomial. For this reason, the treatment of the Gauss linking number in any microscopical model of topologically entangled polymers is complicated. The best strategy to deal with this problem consists in rewriting the delta function $\delta(m_{12}-\chi(\Gamma_1,\Gamma_2))$ as a correlation function of the holonomies of a local field theory, namely the so-called abelian BF-model [56,59,60]

$$\delta(m_{12}-\chi(\Gamma_1,\Gamma_2))=\int\limits_{-\infty}^{+\infty}d\lambda_{12}\,\mathrm{e}^{-i\lambda_{12}m_{12}}\mathcal{Z}_{\mathrm{BF}}(\lambda_{12}) \tag{9}$$

where

$$\begin{aligned}\mathcal{Z}_{\mathrm{BF}}(\lambda_{12})=&\int\mathcal{D}B^{12}_{\mu}(x)\mathcal{D}C^{12}_{\mu}(x)\,\mathrm{e}^{-iS_{\mathrm{BF}}[B,C]}\\&\times\,\mathrm{e}^{-i\tilde{c}_{12}\oint_{\Gamma_1}d\tilde{x}^{\mu}_1(d_1)B^{12}_{\mu}(\tilde{x}_1(d_1))}\,\mathrm{e}^{-i\tilde{d}\oint_{\Gamma_2}d\tilde{x}^{\mu}_2(d_2)C^{12}_{\mu}(\tilde{x}_2(d_2))}.\end{aligned} \tag{10}$$

In the above equation we have put $x\equiv(\boldsymbol{x},t)$ to be dummy integration variables spanning the whole three-dimensional space $\mathbb{R}^3$. Moreover, $S_{\mathrm{BF}}[B,C]$ denotes the action of the abelian BF-model

$$S_{\mathrm{BF}}[B,C]=\frac{\kappa}{4\pi}\int d^3x\,B^{12}_{\mu}(x)\partial_{\nu}C^{12}_{\rho}(x)\epsilon^{\mu\nu\rho}. \tag{11}$$

Above $\epsilon^{\mu\nu\rho}$, $\mu,\nu,\rho=1,2,3$, is the completely antisymmetric ϵ-tensor density defined by the condition $\epsilon^{123}=1$. κ is the coupling constant of the BF-model. Finally, the constants $\tilde{c}_{12}$ and $\tilde{d}$ are given by:

$$\tilde{c}_{12}=\lambda_{12}\qquad\qquad\tilde{d}=\frac{\kappa}{8\pi^2}. \tag{12}$$

While there is some freedom in choosing $\tilde{c}_{12}$ and $\tilde{d}$, one unavoidable requirement in order that Eq. (9) will be satisfied is that one of these parameters should be linearly dependent on κ. In this way, it is easy to check that κ may be completely eliminated from Eq. (10) by performing a rescaling of one of the two fields B^{12}_{μ} and C^{12}_{μ}. This is an expected result, because κ does not appear in the left hand side of Eq. (9), so that it cannot be a new parameter of the theory. By introducing the currents:

$$\zeta^{\mu}_{12}(x)=\tilde{c}_{12}\oint_{\Gamma_1}d\tilde{x}^{\mu}_1(d_1)\delta^{(3)}(x-\tilde{x}_1(d_1))\qquad\qquad\xi^{\mu}_{12}(x)=\tilde{d}\oint_{\Gamma_2}d\tilde{x}^{\mu}_2(d_2)\delta^{(3)}(x-\tilde{x}_2(d_2)) \tag{13}$$

$\mathcal{Z}_{\mathrm{BF}}(\lambda_{12})$ may be rewritten in the more compact way:

$$\mathcal{Z}_{\mathrm{BF}}(\lambda_{12})=\int\mathcal{D}B^{12}_{\mu}(x)\mathcal{D}C^{12}_{\mu}(x)\,\mathrm{e}^{-iS_{\mathrm{BF}}[B,C]}\,\mathrm{e}^{-i\int d^3x\left[\zeta^{\mu}_{12}(x)B^{12}_{\mu}(x)+\xi^{\mu}_{12}(x)C^{12}_{\mu}(x)\right]}. \tag{14}$$

With Eq. (14) the goal of transforming the nonlinear and nonlocal interaction appearing in the right hand side of Eq. (8) is achieved. The right hand side of Eq. (14) represents in fact a local

field theory, the BF-model, interacting with the trajectories Γ_1 and Γ_2. Of course, the price paid for that simplification is the introduction of the fields B^{12}_{μ} and C^{12}_{μ}.

3.2. How to impose constraints on a link composed by plats using the Gauss linking number

In all the above discussion, the two trajectories Γ_1 and Γ_2 have been parametrized with the help of the arc-lengths d_1 and d_2. However, in the present case the loops $\Gamma_1, \ldots, \Gamma_N$ are realized as a set of open paths Γ_{a,I_a} connected together by the conditions (4)–(5). The trajectories Γ_{a,I_a}'s are directed paths $\boldsymbol{r}_{a,I_a}(t_{a,I_a}) = (x^1_{a,I_a}(t_{a,I_a}), x^2_{a,I_a}(t_{a,I_a}))$ parametrized by the variables t_{a,I_a}. This difference of parametrization introduces several important changes. Apart from the fact that we have to deal with many trajectories, also one degree of freedom, represented by the third coordinate $x^3_a(s_a)$, disappears due to the change (135). As a consequence, the method illustrated in the previous Subsection in order to express the Gauss linking number as an amplitude of the BF-model, in particular Eq. (9), should be changed appropriately. Thus, we rewrite the partition function $\mathcal{Z}_{\rm BF}(\lambda_{12})$ of Eq. (10) using the variables t_{a,I_a} to parametrize the trajectories Γ_{a,I_a}. The way in which the curvilinear integrals along the loops Γ_1 and Γ_2 appearing in Eq. (10) should be replaced by integrals over the trajectories Γ_{a,I_a} is shown in Eqs. (133) and (134). As a result, we arrive at the following expression of the partition function $\mathcal{Z}_{\rm BF}(\lambda_{12})$:

$$\mathcal{Z}_{\rm BF}(\lambda_{12}) = \int \mathcal{D}B^{12}_{\mu}(x)\mathcal{D}C^{12}_{\mu}(x)\, \mathrm{e}^{-S_{\rm BF}[B,C]}\, \mathrm{e}^{-i\int d^3x\left[\boldsymbol{\zeta}_{12}(\boldsymbol{x},t)\cdot\boldsymbol{B}^{12}(\boldsymbol{x},t)+\zeta^3_{12}(\boldsymbol{x},t)B^{12}_3(\boldsymbol{x},t)\right]} \times\, \mathrm{e}^{-i\int d^3x\left[\boldsymbol{\xi}_{12}(\boldsymbol{x},t)\cdot\boldsymbol{C}^{12}(\boldsymbol{x},t)+\xi^3_{12}(\boldsymbol{x},t)C^{12}_3(\boldsymbol{x},t)\right]} \tag{15}$$

where $S_{\rm BF}[B,C]$ coincides with the action (11) and

$$\boldsymbol{\zeta}_{12}(\boldsymbol{x},t) = \tilde{c}_{12}\sum_{I_1=1}^{2s_1}\int_{\tau_{1,I_1-1}}^{\tau_{1,I_1}} dt_{1,I_1}\dot{\boldsymbol{r}}_{1,I_1}(t_{1,I_1})\delta^{(2)}(\boldsymbol{x}-\boldsymbol{r}_{1,I_1}(t_{1,I_1}))\delta(t-t_{1,I_1}) \tag{16}$$

$$\boldsymbol{\xi}_{12}(\boldsymbol{x},t) = \tilde{d}\sum_{I_2=1}^{2s_2}\int_{\tau_{2,I_2-1}}^{\tau_{2,I_2}} dt_{2,I_2}\dot{\boldsymbol{r}}_{2,I_2}(t_{2,I_2})\delta^{(2)}(\boldsymbol{x}-\boldsymbol{r}_{2,I_2}(t_{2,I_2}))\delta(t-t_{2,I_2}) \tag{17}$$

$$\zeta^3_{12}(\boldsymbol{x},t) = \tilde{c}_{12}\sum_{I_1=1}^{2s_1}\int_{\tau_{1,I_1-1}}^{\tau_{1,I_1}} dt_{1,I_1}\delta^{(2)}(\boldsymbol{x}-\boldsymbol{r}_{1,I_1}(t_{1,I_1}))\delta(t-t_{1,I_1}) \tag{18}$$

$$\xi^3_{12}(\boldsymbol{x},t) = \tilde{d}\sum_{I_2=1}^{2s_2}\int_{\tau_{2,I_2-1}}^{\tau_{2,I_2}} dt_{2,I_2}\delta^{(2)}(\boldsymbol{x}-\boldsymbol{r}_{2,I_2}(t_{2,I_2}))\delta(t-t_{2,I_2}). \tag{19}$$

3.3. The Coulomb gauge

Now we use the Fourier representation of the topological constraints of Eq. (9), but with the partition function $\mathcal{Z}_{\rm BF}(\lambda_{12})$ written in the form of Eq. (15). In this way the path integral over all conformations of the $2s$-plat can be split into path integrals over all conformations of the trajectories Γ_{a,I_a}. The latter can be regarded as the trajectories of a two-dimensional system of $2s$ particles interacting with abelian BF fields. In order to establish an explicit analogy

between polymers and two-dimensional particles evolving in time, it is convenient to choose a non-covariant gauge like the Coulomb gauge. Similar approaches like that proposed here can be found in [51,57]. Interestingly, in [57] Chern-Simons field theories quantized in noncovariant gauges have also been applied to express the knot and link invariants of $2s$-plats, called in [57] Morse knots. In Refs. [51] and [57] knots and links are however static, they do not fluctuate, and the calculations have been performed in noncovariant gauges different from the Coulomb gauge.

To begin with, we impose the Coulomb gauge condition on the B and C fields

$$\partial^i B_i^{12} = \partial^i C_i^{12} = 0 \tag{20}$$

where $i = 1, 2$ labels the first two components of the vector potentials $B_\mu^{12} = (\boldsymbol{B}^{12}, B_3^{12})$ and $C_\mu^{12} = (\boldsymbol{C}^{12}, C_3^{12})$. After the gauge choice (20), the action of the BF model (11) becomes

$$S_{\mathrm{BF,CG}}[B, C] = \frac{\kappa}{4\pi} \int d^3x \left[B_3^{12} \epsilon^{ij} \partial_i C_j^{12} + C_3^{12} \epsilon^{ij} \partial_i B_j^{12} \right] \tag{21}$$

with $\epsilon^{ij} = \epsilon^{ij3}$ being the two-dimensional completely antisymmetric tensor. The gauge fixing term vanishes in the pure Coulomb gauge where the conditions (20) are strictly satisfied. Also the Faddeev-Popov term, which in principle should be present in Eq. (21), may be neglected because the ghosts decouple from all other fields.

The requirement of transversality of (20) in the "spatial" directions x^1, x^2 implies that the components B_i^{12} and C_i^{12} of the BF fields may be expressed in terms of two scalar fields b^{12} and c^{12} via the Hodge decomposition:

$$B_i^{12} = \epsilon_{ij} \partial^j b^{12} \qquad\qquad C_i^{12} = \epsilon_{ij} \partial^j c^{12}. \tag{22}$$

After performing the above substitutions of fields in the BF action of Eq. (21), we obtain

$$S_{\mathrm{BF,CG}}[B, C] = \frac{\kappa}{4\pi} \int d^3x [B_3^{12} \Delta c^{12} + C_3^{12} \Delta b^{12}]. \tag{23}$$

Now we compute the propagator of the BF fields

$$G_{\mu\nu}(\boldsymbol{x}, t; \boldsymbol{y}, t') = \langle B_\mu^{12}(\boldsymbol{x}, t), C_\nu^{12}(\boldsymbol{y}, t') \rangle. \tag{24}$$

Only the following components of the propagator are different from zero:

$$G_{3i}(\boldsymbol{x}, t; \boldsymbol{y}, t') = \frac{\delta(t - t')}{2\kappa} \epsilon_{ij} \partial_{\boldsymbol{y}}^j \log |\boldsymbol{x} - \boldsymbol{y}|^2 \tag{25}$$

$$G_{i3}(\boldsymbol{x}, t; \boldsymbol{y}, t') = -G_{3i}(\boldsymbol{x}, t; \boldsymbol{y}, t'). \tag{26}$$

The path integration over the scalar fields b^{12} and c^{12} in the partition function $\mathcal{Z}_{\mathrm{BF}}(\lambda)$ is gaussian and can be performed analytically eliminating completely the gauge fields. A natural question that arise at this point is the interpretation of the topological constraint (7) in the Coulomb gauge. As a matter of fact, the BF propagator in the Coulomb gauge breaks explicitly the invariance of the BF model under general three-dimensional transformation. It seems thus hard to recover the form (6) of the Gauss linking number in this gauge. Of course, an equivalent constraint should be obtained in the Coulomb gauge due to gauge invariance. In Appendix C it will be shown by a direct calculation in the case of a 4-plat that this is actually true. The computation of the expression of the equivalent of the Gauss linking number in the Coulomb gauge for a general $2s$-plat is however technically complicated and will not be performed here.

4. The partition function of a plat

4.1. Directed polymers with topological constraints

In order to write the partition function of a $2s$-plat, we follow the strategy explained in the previous Section of dividing each trajectory Γ_a, $a = 1, \ldots, N$, into $2s_a$ open paths Γ_{a,I_a}, $I_a = 1, \ldots, 2s_a$. The statistical sum $\mathcal{Z}_{\text{pol}}(\{m\})$ of the system is performed over all conformations $\boldsymbol{r}_{a,I_a}(t_{a,I_a})$ of the trajectories Γ_{a,I_a} using path integral methods, i.e.:

$$\mathcal{Z}_{\text{pol}}(\{m\}) = \int\limits_{\substack{\text{boundary}\\ \text{conditions}}} \left[\prod_{a=1}^{N}\prod_{I_a=1}^{2s_a} \mathcal{D}\boldsymbol{r}_{a,I_a}(t_{a,I_a})\right] \mathrm{e}^{-(S_{\text{free}}+S_{\text{EV}})} \prod_{a=1}^{N-1}\prod_{b=a+1}^{N} \delta\left(m_{ab} - \chi(\Gamma_a, \Gamma_b)\right). \tag{27}$$

In the above equation the boundary conditions on the trajectories $\boldsymbol{r}_{a,I_a}(t_{a,I_a})$ enforce the constraints (4) and (5). The free part of the action S_{free} is given by

$$S_{\text{free}} = \sum_{a=1}^{N}\sum_{I_a=1}^{2s_a} \int\limits_{\tau_{a,I_a-1}}^{\tau_{a,I_a}} dt_{a,I_a} (-1)^{I_a-1} g_{a,I_a} \left|\frac{d\boldsymbol{r}_{a,I_a}(t_{a,I_a})}{dt_{a,I_a}}\right|^2. \tag{28}$$

The parameters $g_{a,I_a} > 0$ are proportional to the inverse of the Kuhn lengths of the trajectories Γ_{a,I_a}. They are also related to the total lengths of the trajectories Γ_{a,I_a} according to the formula provided in Appendix B. Let us note that S_{free} is a positive definite functional thanks to the factors $(-1)^{I_a-1}$, which compensate the fact that the increment dt_{a,I_a} is negative when I_a is even. The contribution S_{EV} to the total action takes into account the interactions between the monomers which arise because we treat the trajectories Γ_{a,I_a} as directed paths moving in a random media. The mechanism through which these interactions appear after the integration over the non-white random noises is explained in Ref. [61]. Explicitly, S_{EV} is given by

$$\begin{aligned} S_{\text{EV}} = \frac{1}{2}\sum_{a=1}^{N}\sum_{b=1}^{N}\sum_{I_a=1}^{2s_a}\sum_{I_b=1}^{2s_b} \int\limits_{\tau_{a,I_a-1}}^{\tau_{a,I_a}} dt_{a,I_a} \int\limits_{\tau_{b,I_b-1}}^{\tau_{b,I_b}} dt_{b,I_b} (-1)^{I_a+I_b-2} \mathcal{M}^{a,I_a;b,I_b} \\ V\left(\boldsymbol{r}_{a,I_a}(t_{a,I_a}) - \boldsymbol{r}_{b,I_b}(t_{b,I_b})\right) \delta\left(t_{a,I_a} - t_{b,I_b}\right) \end{aligned} \tag{29}$$

where

$$\mathcal{M}^{a,I_a;b,I_b} = \begin{cases} 0 & \text{if } a = b \text{ and } I_a = I_b \\ 1 & \text{otherwise} \end{cases} \tag{30}$$

Due to the matrix $\mathcal{M}^{a,I_a;b,I_b}$ the interactions between a trajectory with itself are forbidden. We note that the presence of the delta functions $\delta\left(t_{a,I_a} - t_{b,I_b}\right)$ is necessary to express the fact that the trajectories Γ_{a,I_a} and Γ_{b,I_b} for $I_a \neq I_b$ may interact only if both t_{a,I_a} and t_{b,I_b} belong to the common interval $[\tau_{a,I_a-1}, \tau_{a,I_a}] \cap [\tau_{b,I_b-1}, \tau_{b,I_b}]$. The potential $V(\boldsymbol{r})$ can be any two-body potential. If the random noises are gaussianly distributed as in Ref. [61], then

$$V(\boldsymbol{r}) = V_0 \delta(\boldsymbol{r}) \tag{31}$$

V_0 being a positive constant. Again, the factors $(-1)^{I_a+I_b-2}$ appearing in S_{EV} are necessary in order to compensate the fact that the increments dt_{a,I_a} and dt_{b,I_b} are negative for even values of

I_a and I_b respectively. Finally, the Dirac delta functions inserted in the right hand side of Eq. (27) impose the topological constraints on each pair of trajectories (Γ_a, Γ_b), $a = 1, \ldots, N-1$, $b = a+1, \ldots, N$.

4.2. Passage to Field Theory I: the topological states

According to Eq. (9), the physically relevant contributions coming from the topological conditions $m_{ab} = \chi(\Gamma_a, \Gamma_b)$, $a = 1, \ldots, N-1$, $b = a+1, \ldots, N$, are encoded in the Fourier transform $\mathcal{Z}_{\rm pol}(\{\lambda\})$ of the original probability function $\mathcal{Z}_{\rm pol}(\{m\})$. Notice that $\mathcal{Z}_{\rm pol}(\{\lambda\})$ is obtained from $\mathcal{Z}_{\rm pol}(\{m\})$ by the relation

$$\mathcal{Z}_{\rm pol}(\{m\}) = \prod_{a=1}^{N-1} \prod_{b=a+1}^{N} \int_{-\infty}^{+\infty} d\lambda_{ab}\, \mathrm{e}^{-i\lambda_{ab} m_{ab}}\, \mathcal{Z}_{\rm pol}(\{\lambda\}). \tag{32}$$

It is easy to realize that

$$\begin{aligned} \mathcal{Z}_{\rm pol}(\{\lambda\}) = \int \left[\prod_{a=1}^{N-1} \prod_{b=a+1}^{N} \mathcal{D}B_\mu^{ab} \mathcal{D}C_\mu^{ab} \right] \mathrm{e}^{-iS_{\rm BF}} \\ \int_{\substack{\text{boundary} \\ \text{conditions}}} \left[\prod_{a=1}^{N} \prod_{I_a=1}^{2s_a} \mathcal{D}\boldsymbol{r}_{a,I_a}(t_{a,I_a}) \right] \mathrm{e}^{-(S_{\rm free}+S_{\rm EV}+S_{\rm top})} \end{aligned} \tag{33}$$

where

$$S_{\rm BF} = \sum_{a=1}^{N-1} \sum_{b=a+1}^{N} \frac{\kappa}{4\pi} \int d^3x\, B_\mu^{ab}(x) \partial_\nu C_\rho^{ab}(x) \epsilon^{\mu\nu\rho} \tag{34}$$

and

$$\begin{aligned} S_{\rm top} = i \sum_{a=1}^{N-1} \sum_{b=a+1}^{N} \lambda_{ab} \sum_{I_a=1}^{2s_a} \int_{\tau_{a,I_a-1}}^{\tau_{a,I_a}} dt_{a,I_a} \Big[\dot{\boldsymbol{r}}_{a,I_a}(t_{a,I_a}) \cdot \boldsymbol{B}^{ab}\left(\boldsymbol{r}_{a,I_a}(t_{a,I_a}), t_{a,I_a}\right) \\ + B_3^{ab}\left(\boldsymbol{r}_{a,I_a}(t_{a,I_a}), t_{a,I_a}\right) \Big] \\ + \frac{i\kappa}{8\pi^2} \sum_{a=1}^{N-1} \sum_{b=a+1}^{N} \sum_{I_b=1}^{2s_b} \int_{\tau_{b,I_b-1}}^{\tau_{b,I_b}} dt_{b,I_b} \Big[\dot{\boldsymbol{r}}_{b,I_b}(t_{b,I_b}) \cdot \boldsymbol{C}^{ab}\left(\boldsymbol{r}_{b,I_b}(t_{b,I_b}), t_{b,I_b}\right) \\ + C_3^{ab}\left(\boldsymbol{r}_{b,I_b}(t_{b,I_b}), t_{b,I_b}\right) \Big]. \end{aligned} \tag{35}$$

After going back to the parametrization of the loops Γ_a with the help of the arc-lengths using Eqs. (133) and (134) and integrating out the BF fields, it is possible to recover in the expression of $\mathcal{Z}_{\rm pol}(\{\lambda\})$ the factors $\prod_{a=1}^{N-1} \prod_{b=a+1}^{N} \mathrm{e}^{+i\lambda_{ab}\chi(\Gamma_a,\Gamma_b)}$ that originate from the Fourier representation of the Dirac delta functions $\prod_{a=1}^{N-1} \prod_{b=a+1}^{N} \delta(m_{ab} - \chi(\Gamma_a, \Gamma_b))$. The integration over the BF fields in $\mathcal{Z}_{\rm pol}(\{\lambda\})$ can be performed applying the formula:

$$\int \prod_{a=1}^{N-1} \prod_{b=a+1}^{N} \mathcal{D}B_{\mu}^{ab}(x)\mathcal{D}C_{\mu}^{ab}(x)\mathrm{e}^{-i(S_{\mathrm{BF}}+S_{\mathrm{top}})} = \prod_{a=1}^{N-1} \prod_{b=a+1}^{N} \mathrm{e}^{+i\lambda_{ab}\chi(\Gamma_a,\Gamma_b)}. \tag{36}$$

Let us note that in the above equation the gauge fields have been quantized using the covariant Lorentz gauge.

4.3. Passage to Field Theory II: the non-topological interactions

Analogously to what has been done in the case of the topological interactions, also the interaction terms in S_{EV} can be made linear and local with the help of auxiliary fields. The strategy to achieve this goal is a straightforward generalization of that followed by de Gennes and coworkers in Refs. [62].

For our purposes, it will be convenient to introduce the set of real scalar fields φ_{a,I_a}, $a = 1,\ldots,N$ and $I_a = 1,\ldots,2s_a$. The action of these fields is

$$S_{\varphi}[J] = S_{\varphi}[0] + i\int d^3x \varphi_{a,I_a}(x)J^{a,I_a}(x) \tag{37}$$

where (here we use the convention that repeated upper and lower indices are summed):

$$S_{\varphi}[0] = \int d^3x d^3y \left[\varphi_{a,I_a}(x)\varphi_{b,I_b}(y)\tilde{V}^{-1}(x-y)(\mathcal{M}^{-1})^{a,I_a;b,I_b}\right] \tag{38}$$

$$\tilde{V}^{-1}(x-y) = V^{-1}(\boldsymbol{x}-\boldsymbol{y})\delta(x^3-y^3) \tag{39}$$

and

$$\int d^2\boldsymbol{y} V(\boldsymbol{x}-\boldsymbol{y})V^{-1}(\boldsymbol{y}-\boldsymbol{z}) = \delta(\boldsymbol{x}-\boldsymbol{z}). \tag{40}$$

In other words, $V^{-1}(\boldsymbol{x}-\boldsymbol{y})$ is the operator that inverts the potential $V(\boldsymbol{r})$ appearing in S_{EV}. The currents $J^{a,I_a}(x)$ are defined as follows

$$J^{a,I_a}(x) = \int_{\tau_{a,I_a-1}}^{\tau_{a,I_a}} dt_{a,I_a}\delta^{(2)}(\boldsymbol{x}-\boldsymbol{r}_{a,I_a}(t_{a,I_a}))\delta(x^3-t_{a,I_a})(-1)^{I_a-1}. \tag{41}$$

$\mathcal{M}^{-1}$ is the inverse of the matrix (we consider a, I_a and b, I_b as composite indexes denoting respectively the rows and columns) defined in Eq. (30).

Supposing that $\mathcal{M}$ is a $n \times n$-dimensional matrix, it is easy to find its inverse, which is given by:

$$\mathcal{M}^{-1} = \begin{pmatrix} \frac{n-2}{n-1} & -\frac{1}{n-1} & \cdots & -\frac{1}{n-1} \\ -\frac{1}{n-1} & \frac{n-2}{n-1} & \cdots & -\frac{1}{n-1} \\ \vdots & \vdots & \ddots & \vdots \\ -\frac{1}{n-1} & -\frac{1}{n-1} & \cdots & \frac{n-2}{n-1} \end{pmatrix} \tag{42}$$

In words, $\mathcal{M}^{-1}$ is the matrix whose diagonal elements are $\frac{n-2}{n-1}$, while all the other elements are $-\frac{1}{n-1}$. Let us note that in the present case $n = N(s_1+s_2+\ldots+s_N)$. It is possible to show that, apart from an irrelevant constant

$$\int \prod_{a=1}^{N} \prod_{I_a=1}^{2s_a} \mathcal{D}\varphi_{a,I_a} \mathrm{e}^{-S_\varphi[J]} = \mathrm{e}^{-S_{\mathrm{EV}}} \tag{43}$$

where S_{EV} is written in the form of Eq. (29).

4.4. Passage to Field Theory III: second quantization

Putting all together, the probability function $\mathcal{Z}_{\mathrm{pol}}(\{\lambda\})$ of Eq. (32) may be expressed in terms of the auxiliary fields $B_\mu^{ab}(x)$, $C_\mu^{ab}(x)$ and $\varphi_{a,I_a}(x)$ as follows

$$\mathcal{Z}_{\mathrm{pol}}(\{\lambda\}) = \int \mathcal{D}(\mathit{fields})\, \mathrm{e}^{-iS_{\mathrm{BF}}}\, \mathrm{e}^{-S_\varphi[0]} \prod_{a=1}^{N} \prod_{I_a=1}^{2s_a} \int \mathcal{D}\boldsymbol{r}_{a,I_a}(t_{a,I_a})\, \mathrm{e}^{-S_{\mathrm{part}}(\boldsymbol{r}_{a,I_a})} \tag{44}$$

where each of the actions $S_{\mathrm{part}}(\boldsymbol{r}_{a,I_a})$, $a = 1, \dots, N$ and $I_a = 1, \dots, 2s_a$, formally coincides with the action of a particle immersed in the external potential $\varphi_{a,I_a}(t_{a,I_a})$ and in an external magnetic field that consists in a linear combination of the fields B_μ^{ab} and C_μ^{ab}:

$$\begin{aligned} S_{\mathrm{part}}(\boldsymbol{r}_{a,I_a}) = \int_{\tau_{a,I_a-1}}^{\tau_{a,I_a}} dt_{a,I_a} \Big[& (-1)^{I_a-1} g_{a,I_a} \dot{\boldsymbol{r}}_{a,I_a}^2(t_{a,I_a}) + i\varphi_{a,I_a}(\boldsymbol{r}_{a,I_a}(t_{a,I_a}), t_{a,I_a})(-1)^{I_a-1} \\ & + i\dot{\boldsymbol{r}}_{a,I_a}(t_{a,I_a}) \cdot \boldsymbol{A}^a(\boldsymbol{r}_{a,I_a}(t_{a,I_a}), t_{a,I_a}) + iA_3^a(\boldsymbol{r}_{a,I_a}(t_{a,I_a}), t_{a,I_a}) \Big]. \end{aligned} \tag{45}$$

In Eq. (45) we have put

$$A_\mu^1(\boldsymbol{r}, t) = \sum_{b=2}^{N} \lambda_{1b} B_\mu^{1b}(\boldsymbol{r}, t) \tag{46}$$

$$A_\mu^a(\boldsymbol{r}, t) = \sum_{b=a+1}^{N} \lambda_{ab} B_\mu^{ab}(\boldsymbol{r}, t) + \frac{\kappa}{8\pi^2} \sum_{c=1}^{a-1} C_\mu^{ca}(\boldsymbol{r}, t) \qquad a = 2, \dots, N-1 \tag{47}$$

$$A_\mu^N(\boldsymbol{r}, t) = \frac{\kappa}{8\pi^2} \sum_{c=1}^{N-1} C_\mu^{cN}(\boldsymbol{r}, t) \tag{48}$$

and

$$\mathcal{D}(\mathit{fields}) = \left[\prod_{a=1}^{N-1} \prod_{b=a+1}^{N} \int \mathcal{D}B_\mu^{ab} C_\mu^{ab} \right] \left[\prod_{a=1}^{N} \prod_{I_a=1}^{2s_a} \int \mathcal{D}\varphi_{a,I_a} \right]. \tag{49}$$

Let us note that with Eq. (44) we have succeeded to rewrite the probability function $\mathcal{Z}_{\mathrm{pol}}(\{\lambda\})$ in such a way that the trajectories $\boldsymbol{r}_{a,I_a}(t_{a,I_a})$ do not interact directly with each other. They interact only indirectly via the fields φ_{a,I_a} and A_μ^a.

The problem of passing to second quantized path integral in the case of a particle with partition function:

$$\mathcal{Z}_{\mathrm{part}}^{a,I_a} = \int \mathcal{D}\boldsymbol{r}_{a,I_a}(t_{a,I_a})\, \mathrm{e}^{-S_{\mathrm{part}}(\boldsymbol{r}_{a,I_a})} \tag{50}$$

is very well known in polymer physics [53,56,59,63]. After introducing n_{a,I_a}-multiplets of complex replica fields:

$$\vec{\Psi}(\boldsymbol{x},t) = (\psi^{1}_{a,I_a}(\boldsymbol{x},t),\ldots,\psi^{n_{a,I_a}}_{a,I_a}(\boldsymbol{x},t)) \tag{51}$$

$$\vec{\Psi}^{*}(\boldsymbol{x},t) = (\psi^{1*}_{a,I_a}(\boldsymbol{x},t),\ldots,\psi^{*n_{a,I_a}}_{a,I_a}(\boldsymbol{x},t)) \tag{52}$$

we obtain

$$\mathcal{Z}^{a,I_a}_{\rm part} = \lim_{n_{a,I_a}\to 0}\int \mathcal{D}\vec{\Psi}_{a,I_a}\mathcal{D}\vec{\Psi}^{*}_{a,I_a}\psi^{1*}_{a,I_a}(\boldsymbol{r}_{a,I_a}(\tau_{a,I_a}),\tau_{a,I_a}) \psi^{1}_{a,I_a}(\boldsymbol{r}_{a,I_a}(\tau_{a,I_a}-1),\tau_{a,I_a}-1)\,{\rm e}^{-S_{\rm part}(\vec{\Psi}^{*}_{a,I_a},\vec{\Psi}_{a,I_a})} \tag{53}$$

where

$$\begin{aligned} S_{\rm part}(\vec{\Psi}^{*}_{a,I_a},\vec{\Psi}_{a,I_a}) = \int_{\tau_{a,I_a}-1}^{\tau_{a,I_a}} dt_{a,I_a}\int d^2\boldsymbol{x}\Bigg[& \vec{\Psi}^{*}_{a,I_a}\frac{\partial}{\partial t}\vec{\Psi}_{a,I_a} \\ & + \frac{1}{4g_{a,I_a}}\left|\left(\nabla - i(-1)^{I_a-1}\boldsymbol{A}^{a}\right)\vec{\Psi}_{a,I_a}\right|^2 \\ & + i\left|\vec{\Psi}_{a,I_a}\right|^2\left(A^{a}_{3} + \varphi_{a,I_a}(-1)^{I_a-1}\right)\Bigg]. \end{aligned} \tag{54}$$

In writing Eq. (54) and in all the formulas below we follow the convention that, whenever products of $\vec{\Psi}^{*}_{a,I_a}$ with $\vec{\Psi}_{a,I_a}$ appear, also the scalar product over the replica multiplets is implicitly understood.

Eventually, the probability function $\mathcal{Z}_{\rm pol}(\{\lambda\})$ of Eq. (44) becomes

$$\mathcal{Z}_{\rm pol}(\{\lambda\}) = \int \mathcal{D}(\textit{fields})\,{\rm e}^{-iS_{\rm BF}}\,{\rm e}^{-S_{\varphi}[0]}\prod_{a=1}^{N}\prod_{I_a=1}^{2s_a}\mathcal{Z}^{a,I_a}_{\rm part} \tag{55}$$

with $\mathcal{Z}^{a,I_a}_{\rm part}$ given by Eq. (53). From the actions $S_{\rm part}(\vec{\Psi}^{*}_{a,I_a},\vec{\Psi}_{a,I_a})$ shown in Eq. (54), we see that the topological forces are tightly related to the non-topological forces mediated by the potential $V(\boldsymbol{x}-\boldsymbol{y})$. This can be realized from the fact that the fields φ_{a,I_a} and the third component of the vector fields A^{a}_{3} are coupled in the same way with the matter fields $\vec{\Psi}_{a,I_a}$ and $\vec{\Psi}^{*}_{a,I_a}$. This interplay between topological and non-topological interactions remains explicit after the integration over the auxiliary φ_{a,I_a}. After performing these integrations, we arrive at the final expression of $\mathcal{Z}_{\rm pol}(\{\lambda\})$:

$$\begin{aligned} \mathcal{Z}_{\rm pol}(\{\lambda\}) = & \left[\prod_{c=1}^{N-1}\prod_{d=c+1}^{N}\int \mathcal{D}B^{cd}_{\mu}\mathcal{D}C^{cd}_{\mu}\right] \\ & \left[\prod_{a=1}^{N}\prod_{I_a=1}^{2s_a}\lim_{n_{a,I_a}\to 0}\int \mathcal{D}\vec{\Psi}^{*}_{a,I_a}\mathcal{D}\vec{\Psi}_{a,I_a}\psi^{1*}_{a,I_a}(\boldsymbol{r}_{a,I_a}(\tau_{a,I_a}),\tau_{a,I_a})\right. \\ & \left.\psi^{1}_{a,I_a}(\boldsymbol{r}_{a,I_a}(\tau_{a,I_a}-1),\tau_{a,I_a}-1)\right]{\rm e}^{-iS_{\rm BF}}\,{\rm e}^{-S_{\rm matter}} \end{aligned} \tag{56}$$

where $S_{\rm BF}$ has been already defined in Eq. (33) and

$$S_{\rm matter} = S^{1}_{\rm matter} + S^{2}_{\rm matter} \tag{57}$$

with

$$S^1_{\text{matter}} = \sum_{a=1}^{N} \sum_{I_a=1}^{2s_a} \int_{\tau_{a,I_a-1}}^{\tau_{a,I_a}} dt_{a,I_a} \int d^2\boldsymbol{x} \left[\vec{\Psi}^*_{a,I_a} \left(\frac{\partial}{\partial t} + i A^a_3 \right) \vec{\Psi}_{a,I_a} + \frac{1}{4g_{a,I_a}} \left| \left(\boldsymbol{\nabla} - i(-1)^{I_a-1} \boldsymbol{A}^a \right) \vec{\Psi}_{a,I_a} \right|^2 \right] \tag{58}$$

and

$$S^2_{\text{matter}} = \sum_{a,b=1}^{N} \sum_{I_a=1}^{2s_a} \sum_{I_b=1}^{2s_b} \int_{\tau_{a,I_a-1}}^{\tau_{a,I_a}} dt_{a,I_a} \int d^2\boldsymbol{x} d^2\boldsymbol{y} \times \frac{\mathcal{M}^{a,I_a;b,I_b}}{4} \left| \vec{\Psi}_{a,I_a}(\boldsymbol{x},t) \right|^2 V(\boldsymbol{x}-\boldsymbol{y}) \left| \vec{\Psi}_{b,I_b}(\boldsymbol{y},t) \right|^2 . \tag{59}$$

Looking at Eqs. (56)–(59), we see that the original polymer partition function (33) has been transformed into a field theory of two-dimensional quasiparticles. The action S^1_{matter} in Eq. (58) is formally equivalent to the action of a multicomponent system of anyons subjected to the interactions described by the action S^2_{matter} in Eq. (59). Similar systems have been discussed in connection with the fractional quantum Hall effect and high-T_C superconductivity [64]. The only differences in our case are the boundaries of the integrations over the time, which in this work depend on the heights of the points of maxima and minima of the two trajectories $\Gamma_1, \ldots, \Gamma_N$. Moreover, here the quasiparticles are bosons of spin n_{a,I_a}, $a = 1, \ldots, N$ and $I_a = 1, \ldots, 2s_a$ considered in the limit $n_{a,I_a} \to 0$.

At this point, we quantize the BF fields using the Coulomb gauge and perform the integration over the third components B^{ab}_3 and C^{ab}_3. The generalization of Eq. (23) to the case of N loops $\Gamma_1, \ldots, \Gamma_N$ is straightforward. The BF action S_{BF} becomes in the Coulomb gauge:

$$S_{\text{BF}} = \sum_{a=1}^{N-1} \sum_{b=a+1}^{N} \frac{\kappa}{4\pi} \int d^2\boldsymbol{x} dt \left[B^{ab}_3 \Delta c^{ab} + C^{ab}_3 \Delta b^{ab} \right] \tag{60}$$

where b^{ab} and c^{ab} are scalar fields related to the Hodge decomposition (22). The third components of the BF fields play the role of Lagrange multipliers. They can be easily integrated out in the probability function $\mathcal{Z}_{\text{pol}}(\{\lambda\})$ of Eq. (56). As a result of this operation, the following constraints are imposed:

$$\frac{\kappa}{4\pi} \Delta c^{ab} + \lambda_{ab} \sum_{I_a=1}^{2s_a} |\vec{\Psi}_{a,I_a}|^2 \theta(\tau_{a,I_a} - t)\theta(t - \tau_{a,I_a-1}) = 0 \quad \begin{cases} a = 1, \ldots, N-1 \\ b = 2, \ldots, N \end{cases} \tag{61}$$

$$\Delta b^{ab} + \frac{1}{2\pi} \sum_{I_b=1}^{2s_b} |\vec{\Psi}_{b,I_b}|^2 \theta(\tau_{b,I_b} - t)\theta(t - \tau_{b,I_b-1}) = 0 \quad \begin{cases} b = 2, \ldots, N \\ a = 1, \ldots, b-1 \end{cases} \tag{62}$$

The final form of the probability function $\mathcal{Z}_{\text{pol}}(\{\lambda\})$ in the Coulomb gauge is

$$\mathcal{Z}_{\text{pol}}(\{\lambda\}) = \left[\prod_{c=1}^{N-1} \prod_{d=c+1}^{N} \int \mathcal{D}\boldsymbol{B}^{cd} \mathcal{D}\boldsymbol{C}^{cd} \right]$$

$$\times \left[\prod_{a=1}^{N} \prod_{I_a=1}^{2s_a} \lim_{n_{a,I_a}\to 0} \int \mathcal{D}\vec{\Psi}^{*}_{a,I_a} \mathcal{D}\vec{\Psi}_{a,I_a} \psi^{1*}_{a,I_a}(\boldsymbol{r}_{a,I_a}(\tau_{a,I_a}),\tau_{a,I_a}) \psi^{1}_{a,I_a}(\boldsymbol{r}_{a,I_a}(\tau_{a,I_a}),\tau_{a,I_a}) \right]$$
$$\times \mathrm{e}^{-S_{\mathrm{matter,CG}}} \tag{63}$$

where

$$S_{\mathrm{matter,CG}} = S^{1}_{\mathrm{matter,CG}} + S^{2}_{\mathrm{matter}}. \tag{64}$$

Here S^{2}_{matter} is the same of Eq. (59) while

$$S^{1}_{\mathrm{matter,CG}} = \sum_{a=1}^{N} \sum_{I_a=1}^{2s_a} \int_{\tau_{a,I_a-1}}^{\tau_{a,I_a}} dt_{a,I_a} \int d^2\boldsymbol{x} \frac{1}{4g_{a,I_a}} \Big[|\nabla \vec{\Psi}_{a,I_a}|^2 + i(-1)^{I_a-1} \boldsymbol{A}^a \cdot \boldsymbol{J}^a + |\vec{\Psi}_{a,I_a}|^2 (\boldsymbol{A}^a)^2 \Big]. \tag{65}$$

In the above equation the $\boldsymbol{J}^a$'s are the currents

$$\boldsymbol{J}^a = \vec{\Psi}_{a,I_a} \nabla \vec{\Psi}^{*}_{a,I_a} - \vec{\Psi}^{*}_{a,I_a} \nabla \vec{\Psi}_{a,I_a}. \tag{66}$$

The BF-fields cease to be independent degrees of freedom because, thanks to the constraints (61)–(62), they can be expressed as functions of the matter fields $\vec{\Psi}^{*}_{a,I_a}$, $\vec{\Psi}_{a,I_a}$. As a matter of fact, these constraints can be solved analytically with respect to the remnants b^{ab}, c^{ab} of the original gauge fields. Remembering that $B^{ab}_{i} = \epsilon_{ij}\partial^j b^{ab}$ and $C^{ab}_{i} = \epsilon_{ij}\partial^j c^{ab}$, we write down directly the components of the fields $\boldsymbol{B}^{ab}$ and $\boldsymbol{C}^{ab}$:

$$C^{ab}_{i}(\boldsymbol{x},t) = -\frac{2\lambda_{ab}}{\kappa} \int d^2\boldsymbol{y} \sum_{I_a=1}^{2s_a} |\vec{\Psi}_{a,I_a}(\boldsymbol{y},t)|^2 \epsilon_{ij} \frac{(x-y)^j}{|\boldsymbol{x}-\boldsymbol{y}|^2} \theta(\tau_{a,I_a}-t)\theta(t-\tau_{a,I_a-1})$$
$$= 0, \qquad a = 1,\ldots,N-1, \quad b = 2,\ldots,N, \tag{67}$$

$$B^{ab}_{i}(\boldsymbol{x},t) = -\int d^2\boldsymbol{y} \frac{1}{4\pi^2} \epsilon_{ij} \frac{(x-y)^j}{|\boldsymbol{x}-\boldsymbol{y}|^2} \sum_{I_b=1}^{2s_b} |\vec{\Psi}_{b,I_b}(\boldsymbol{y},t)|^2 \theta(\tau_{b,I_b}-t)\theta(t-\tau_{b,I_b-1})$$
$$= 0, \qquad b = 2,\ldots,N, \quad a = 1,\ldots,b-1. \tag{68}$$

The above expressions of the BF-field should be inserted in Eqs. (46)–(48) which define the fields $\boldsymbol{A}^a$ appearing in the action (58). Let us note that the fields $\boldsymbol{A}^a$ written in terms of the solutions (67)–(68) do not contain the parameter κ as expected. Putting all together, it is possible to conclude that the total energy density of the system of plats contains quartic and sextic interactions in the matter fields $\vec{\Psi}^{*}_{a,I_a}$, $\vec{\Psi}_{a,I_a}$. This conclusion is in agreement with previous calculations performed in [55], where it has been shown that the topological constraints generate quartic and sextic corrections due to the presence of the topological constraints. The difference is that in [55] the approximate method of the effective potential has been used, while the present calculations are exact.

5. A statistical model of a $2s$-plat composed by N-linked polymers

Using Feynman diagrams, the nontopological quartic interactions in Eq. (59) may be represented by the four-vertex in Fig. 6-(a). The quartic interactions of topological origin described

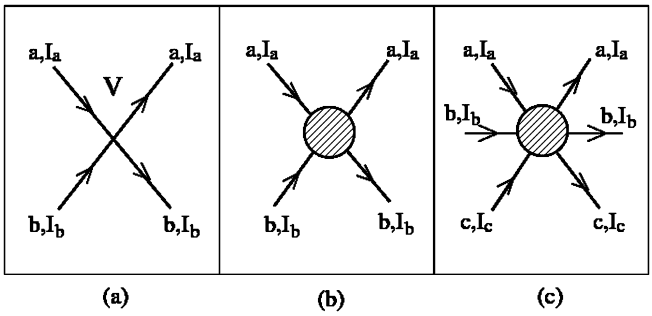

Fig. 6. Feynman diagram representation of the interactions in Eqs. (59) and (65).

by the contributions to $S^1_{\text{matter,CG}}$ of Eq. (65) in which the fields $\boldsymbol{A}^a$ are coupled to the currents $\boldsymbol{J}^a$, correspond to the four-vertex of Fig. 6-(b). The sextic interactions, also of topological origin, consisting in the terms in $S^1_{\text{matter,CG}}$ proportional to $(\boldsymbol{A}^a)^2$, are displayed in Fig. 6-(c). Let us note that in both the four-vertex and the six-vertex of Figs. 6-(b) and 6-(c) the external legs depart from a solid circle. This circle symbolizes the fact that these vertices contain non-perturbative contributions coming from the path integral summation over the field B^{ab}_μ and C^{ab}_μ. The strengths g_4 and g_6 of the quartic and sextic interactions of topological origin are respectively proportional to:

$$g_4 \sim \frac{\lambda_{ab}}{8\pi^2} \qquad\qquad g_6 \sim \frac{\lambda_{ab}\lambda_{ac}}{16\pi^4} \tag{69}$$

As it is clear from Eq. (8), the λ_{ab}'s are Fourier coefficients varying in the interval $(-\infty, +\infty)$. For this reason, g_4 and g_6 cannot be considered as real coupling constant. However, the parameters λ_{ab} may be interpreted as chemical potentials that specify how easy is the linking of two trajectories Γ_a and Γ_b. To small values of λ_{ab} correspond big values of the linking number m_{ab} and viceversa.

An important feature of the model described in Eqs. (63) and (64) is that the interactions of topological origin have sextic interactions, in which the monomers of three different loops are involved. The appearance of three-body forces was up to now not supposed to be possible in the case of topological constraints imposed using the Gauss linking number. As a matter of fact, this link invariant controls only the linking between pairs of polymer rings. In the case $N = 2$, in which we have just two loops, these three-body interactions are suppressed as showed in Ref. [55], because they vanish when the limit in which the numbers of replicas n_{a,I_a} approach zero is performed in the probability function of Eq. (63). However, not all diagrams with three-body interactions disappear when $N > 2$. An example of nontrivial contribution in which interactions of three monomers are taking place is shown in Fig. 7.

Another characteristic of the model describing the statistical mechanics of $2s$-plats introduced here is the existence of vortex solutions of the equations that minimize the energy of the static field configurations. An example of such solutions will be presented in the next Section in the case $N = 2$.

6. Self-dual solutions of the two-polymer problem

In this Section we restrict ourselves for simplicity to 4-plats. Moreover, the non-topological interactions contained in S^2_{matter} will be ignored. We will also suppose that the replica numbers are independent of I_a, i.e.:

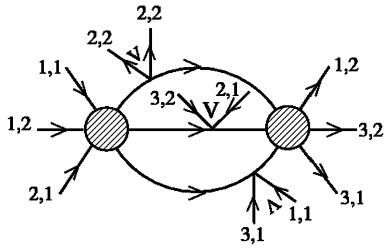

Fig. 7. Example of a process in which the three body interactions of topological origin do not vanish in the zero replicas limit $n_{a,I_a} \to 0$ appearing in Eq. (63). The process describes the interaction of the trajectories Γ_{a,I_a}, $a = 1, 2, 3$, $I_a = 1, 2$ forming a 6-plat in which three loops $\Gamma_1, \Gamma_2, \Gamma_3$ are linked together.

$$\vec{\Psi}(\boldsymbol{x}, t) = (\psi^1_{a,I_a}(\boldsymbol{x}, t), \ldots, \psi^{n_a}_{a,I_a}(\boldsymbol{x}, t)) \qquad a = 1, 2 \text{ and } I_a = 1, 2 \tag{70}$$

$$\vec{\Psi}^*(\boldsymbol{x}, t) = (\psi^{1*}_{a,I_a}(\boldsymbol{x}, t), \ldots, \psi^{*n_a}_{a,I_a}(\boldsymbol{x}, t)) \qquad a = 1, 2 \text{ and } I_a = 1, 2. \tag{71}$$

In Eqs. (51) and (52) each pair of complex fields $\vec{\Psi}^*_{a,I_a}, \vec{\Psi}_{a,I_a}$ had a separate replica index n_{a,I_a}, but it is easy to check that I_a-independent replica indexes are possible too without jeopardizing the passage to field theory and in particular the calculations made in Section 4. The partition function of a 4-plat formed by two linked polymers is obtained by putting $N = 2$ and $s_1 = s_2 = 1$ in the general partition function of a $2s$-plat given in Eq. (63). Accordingly, the action $S_{\text{matter,CG}}$ in Eq. (64) in this particular case becomes

$$\begin{aligned} S_{\text{matter,CG}} = & \int_{\tau_{1,0}}^{\tau_{1,1}} dt \int d^2\boldsymbol{x} \Bigg\{ \vec{\Psi}^*_{1,1} \left[\frac{\partial}{\partial t} - \frac{1}{4g_{1,1}} \boldsymbol{D}^2 \left(-\lambda_{12}, \boldsymbol{B}^{12} \right) \right] \vec{\Psi}_{1,1} \\ & + \vec{\Psi}^*_{1,2} \left[\frac{\partial}{\partial t} - \frac{1}{4g_{1,2}} \boldsymbol{D}^2 \left(\lambda_{12}, \boldsymbol{B}^{12} \right) \right] \vec{\Psi}_{1,2} \Bigg\} \\ & + \int_{\tau_{2,0}}^{\tau_{2,1}} dt \int d^2\boldsymbol{x} \vec{\Psi}^*_{2,1} \Bigg\{ \left[\frac{\partial}{\partial t} - \frac{1}{4g_{2,1}} \boldsymbol{D}^2 \left(-\frac{\kappa}{8\pi^2}, \boldsymbol{C}^{12} \right) \right] \vec{\Psi}_{2,1} \\ & + \vec{\Psi}^*_{2,2} \left[\frac{\partial}{\partial t} - \frac{1}{4g_{2,2}} \boldsymbol{D}^2 \left(\frac{\kappa}{8\pi^2}, \boldsymbol{C}^{12} \right) \right] \vec{\Psi}_{2,2} \Bigg\}. \end{aligned} \tag{72}$$

In the above equation $\boldsymbol{D}$ denotes the covariant derivatives, which are of two types depending if they are defined with respect to the field $\boldsymbol{B}^{12}$ or to the field $\boldsymbol{C}^{12}$:

$$\boldsymbol{D}(\pm\lambda_{12}, \boldsymbol{B}^{12}) = \nabla \pm i\lambda_{12}\boldsymbol{B}^{12} \qquad \boldsymbol{D}\left(\pm\frac{\kappa}{8\pi^2}, \boldsymbol{C}^{12} \right) = \nabla \pm i\frac{\kappa}{8\pi^2}\boldsymbol{C}^{12}. \tag{73}$$

As mentioned at the end of the previous Section, the fields $\boldsymbol{B}^{12}$ and $\boldsymbol{C}^{12}$ are not independent degrees of freedom, because they are fully determined by the constraints (61)–(62). In the present case $N = 2$, $s_1 = s_2 = 2$, the required conditions are:

$$\epsilon^{ij}\partial_i B^{12}_j = -\frac{1}{2\pi} \left(|\vec{\Psi}_{21}|^2 + |\vec{\Psi}_{22}|^2 \right) \theta(\tau_{2,1} - t)\theta(t - \tau_{2,0}) \tag{74}$$

$$\epsilon^{ij}\partial_i C^{12}_j = -\frac{4\pi\lambda_{12}}{\kappa} \left(|\vec{\Psi}_{11}|^2 + |\vec{\Psi}_{12}|^2 \right) \theta(\tau_{1,1} - t)\theta(t - \tau_{1,0}). \tag{75}$$

We will consider now the static field configurations that minimize the action $S_{\text{matter,CG}}$ of Eq. (72). From Ref. [42] it is known that this action admits self-dual solutions in the case in which the parameters g_{a,I_a}, $a = 1, 2$ and $I_a = 1, 2$ are all equal. To this purpose, for any constant γ and gauge field $\boldsymbol{a}$ we define the new covariant derivatives $D_\pm(\gamma, \boldsymbol{a})$:

$$D_\pm(\gamma, \boldsymbol{a}) = D_1(\gamma, \boldsymbol{a}) \pm i D_2(\gamma, \boldsymbol{a}) \tag{76}$$

where D_1 and D_2 denote the first and second components of the covariant derivative $\boldsymbol{D}$. In terms of the $D_\pm$'s, the self-duality equations may be expressed as follows:

$$D_+\left(-\lambda_{12}, \boldsymbol{B}^{12}\right)\psi_{1,1}^{n_1} = 0 \tag{77}$$

$$D_+\left(\lambda_{12}, \boldsymbol{B}^{12}\right)\psi_{1,2}^{n_1} = 0 \tag{78}$$

$$D_-\left(-\frac{\kappa}{8\pi^2}, \boldsymbol{C}^{12}\right)\psi_{2,1}^{n_2} = 0 \tag{79}$$

$$D_-\left(\frac{\kappa}{8\pi^2}, \boldsymbol{C}^{12}\right)\psi_{2,2}^{n_2} = 0. \tag{80}$$

We notice in the constraints (74) and (75) the cumbersome presence of the Heaviside θ-functions. They are required in order to take into account the fact that the heights of the points belonging to the trajectories Γ_{a,I_a} are only partially overlapping. As a consequence, to avoid complications, we will assume that $\tau_{1,0} = \tau_{2,0} = \tau_0$ and $\tau_{1,1} = \tau_{2,1} = \tau_1$, i.e. all trajectories will start and end at the same height. In this way the Heaviside θ-functions are no longer needed. Moreover, we will restrict ourselves to replica symmetric solutions by putting:

$$\begin{aligned}
&\psi^1_{1,I_1} = \cdots = \psi^{n_1}_{1,I_1} = \psi_{1,I_1} \quad \text{for} \quad I_1 = 1, 2 \\
&\psi^1_{2,I_2} = \cdots = \psi^{n_2}_{2,I_2} = \psi_{2,I_2} \quad \text{for} \quad I_2 = 1, 2.
\end{aligned} \tag{81}$$

After these simplifications, the self-duality conditions (77)–(80) and the constraints (74) and (75) become:

$$\left[\partial_1 - i\lambda_{12}B_1^{12} + i\left(\partial_2 - i\lambda_{12}B_2^{12}\right)\right]\psi_{1,1} = 0 \tag{82}$$

$$\left[\partial_1 + i\lambda_{12}B_1^{12} + i\left(\partial_2 + i\lambda_{12}B_2^{12}\right)\right]\psi_{1,2} = 0 \tag{83}$$

$$\left[\partial_1 - \frac{i\kappa}{8\pi^2}C_1^{12} - i\left(\partial_2 - \frac{i\kappa}{8\pi^2}C_2^{12}\right)\right]\psi_{2,1} = 0 \tag{84}$$

$$\left[\partial_1 + \frac{i\kappa}{8\pi^2}C_1^{12} - i\left(\partial_2 + \frac{i\kappa}{8\pi^2}C_2^{12}\right)\right]\psi_{2,2} = 0 \tag{85}$$

and

$$\epsilon^{ij}\partial_i B_j^{12} = -\frac{1}{2\pi}n_2\left(|\psi_{2,1}|^2 + |\psi_{2,2}|^2\right) \tag{86}$$

$$\epsilon^{ij}\partial_i C_j^{12} = -\frac{4n_1\pi\lambda_{12}}{\kappa}\left(|\psi_{1,1}|^2 + |\psi_{1,2}|^2\right). \tag{87}$$

At this point we pass to polar coordinates by performing the transformations:

$$\psi_{a,I_a} = \mathrm{e}^{i\omega_{a,I_a}}\rho_{a,I_a}^{1/2}. \tag{88}$$

After the above change of variables in Eqs. (82)–(87) and separating the real and imaginary parts, we obtain:

$$\partial_1\omega_{1,1} - \lambda_{12}B_1^{12} + \frac{1}{2}\partial_2 \log\rho_{1,1} = 0 \tag{89}$$

$$-\partial_2\omega_{1,1} + \lambda_{12}B_2^{12} + \frac{1}{2}\partial_1 \log\rho_{1,1} = 0 \tag{90}$$

$$\partial_1\omega_{1,2} + \lambda_{12}B_1^{12} + \frac{1}{2}\partial_2 \log\rho_{1,2} = 0 \tag{91}$$

$$-\partial_2\omega_{1,2} - \lambda_{12}B_2^{12} + \frac{1}{2}\partial_1 \log\rho_{1,2} = 0 \tag{92}$$

$$\partial_1\omega_{2,1} - \frac{\kappa}{8\pi^2}C_1^{12} - \frac{1}{2}\partial_2 \log\rho_{2,1} = 0 \tag{93}$$

$$\partial_2\omega_{2,1} - \frac{\kappa}{8\pi^2}C_2^{12} + \frac{1}{2}\partial_1 \log\rho_{2,1} = 0 \tag{94}$$

$$\partial_1\omega_{2,2} + \frac{\kappa}{8\pi^2}C_1^{12} - \frac{1}{2}\partial_2 \log\rho_{2,2} = 0 \tag{95}$$

$$\partial_2\omega_{2,2} + \frac{\kappa}{8\pi^2}C_2^{12} + \frac{1}{2}\partial_1 \log\rho_{2,2} = 0 \tag{96}$$

$$\epsilon^{ij}\partial_i B_j = -\frac{1}{2\pi}n_2\left(\rho_{2,1} + \rho_{2,2}\right) \tag{97}$$

$$\epsilon^{ij}\partial_i C_j = -\frac{4n_1\pi\lambda_{12}}{\kappa}\left(\rho_{1,1} + \rho_{1,2}\right). \tag{98}$$

To solve equations (89)–(96) with respect to the unknowns ω_{a,I_a} and ρ_{a,I_a}, we proceed as follows. First of all, we isolate from Eq. (89) and Eq. (91) the same quantity $\lambda_{12}B_1^{12}$. By requiring that the expressions of $\lambda_{12}B_1^{12}$ provided by Eqs. (89) and (91) are equal, we obtain the consistency condition

$$\partial_1\omega_{1,1} + \frac{1}{2}\partial_2 \log\rho_{1,1} = -\partial_1\omega_{1,2} - \frac{1}{2}\partial_2 \log\rho_{1,2} \tag{99}$$

A possible solution of Eq. (99) is

$$\omega_{1,1} = -\omega_{1,2} \quad \text{and} \quad \rho_{1,1} = \frac{A_1}{\rho_{1,2}} \tag{100}$$

where A_1 is at most a function of x^1. As well, we require that the two different expressions of the quantity $\lambda_{12}B_2^{12}$ obtained from Eqs. (90) and (92) are equal. On this way one obtains a condition analogous to (99), which may be solved by applying the ansatz (100) and additionally requiring that A_1 is a constant. In a similar way, it is possible to extract from equations (93)–(96) the conditions:

$$\omega_{2,1} = -\omega_{2,2} \quad \text{and} \quad \rho_{2,1} = \frac{A_2}{\rho_{2,2}} \tag{101}$$

with A_2 being a constant.

Thanks to Eqs. (100) and (101), the number of unknowns to be computed is reduced. For instance, if we choose as independent degrees of freedom $\omega_{1,1}$, $\omega_{2,1}$, $\rho_{1,1}$ and $\rho_{2,1}$, the remaining classical field configurations $\omega_{1,2}$, $\omega_{2,2}$, $\rho_{1,2}$ and $\rho_{2,2}$ can be derived using such equations. As a consequence, the system of equations (89)–(98) reduces to:

$$\lambda_{12} B_1^{12} = \partial_1 \omega_{1,1} + \frac{1}{2} \partial_2 \log \rho_{1,1} \tag{102}$$

$$\lambda_{12} B_2^{12} = \partial_2 \omega_{1,1} - \frac{1}{2} \partial_1 \log \rho_{1,1} \tag{103}$$

$$\frac{\kappa}{8\pi^2} C_1^{12} = \partial_1 \omega_{2,1} - \frac{1}{2} \partial_2 \log \rho_{2,1} \tag{104}$$

$$\frac{\kappa}{8\pi^2} C_2^{12} = \partial_2 \omega_{2,1} + \frac{1}{2} \partial_1 \log \rho_{2,1} \tag{105}$$

$$\partial_1 B_2^{12} - \partial_2 B_1^{12} = -\frac{1}{2\pi} n_2 \left(\rho_{2,1} + \frac{A_2}{\rho_{2,1}} \right) \tag{106}$$

$$\partial_1 C_2^{12} - \partial_2 C_1^{12} = -\frac{4 n_1 \pi \lambda_{12}}{\kappa} \left(\rho_{1,1} + \frac{A_1}{\rho_{1,1}} \right) \tag{107}$$

where we have used the fact that $\epsilon^{ij} \partial_i B_j = \partial_1 B_2^{12} - \partial_2 B_1^{12}$ and $\epsilon^{ij} \partial_i C_j = \partial_1 C_2^{12} - \partial_2 C_1^{12}$. Eqs. (102)–(107) contain the unknowns $\omega_{1,1}$, $\omega_{2,1}$, $\rho_{1,1}$ and $\rho_{2,1}$ that will be determined below.

By subtracting term by term the two equations resulting from the derivation of Eqs. (102) and (103) with respect to the variables x^2 and x^1 respectively, we obtain as an upshot the relation:

$$\lambda_{12} \left(\partial_1 B_2^{12} - \partial_2 B_1^{12} \right) = \partial_1 \partial_2 \omega_{1,1} - \partial_2 \partial_1 \omega_{1,1} - \frac{1}{2} \Delta \log \rho_{1,1} \tag{108}$$

with $\Delta = \partial_1^2 + \partial_2^2$ being the two-dimensional Laplacian.

Assuming that $\omega_{1,1}$ is a regular function satisfying the relation

$$\partial_1 \partial_2 \omega_{1,1} - \partial_2 \partial_1 \omega_{1,1} = 0 \tag{109}$$

Eq. (108) becomes:

$$\lambda_{12} \left(\partial_1 B_2^{12} - \partial_2 B_1^{12} \right) = -\frac{1}{2} \Delta \log \rho_{1,1} . \tag{110}$$

An analogous identity can be derived starting from Eqs. (104) and (105):

$$\frac{\kappa}{4\pi^2} \left(\partial_1 C_2^{12} - \partial_2 C_1^{12} \right) = \Delta \log \rho_{2,1} . \tag{111}$$

The compatibility of (110) and (111) with the constraints (106) and (107) respectively leads to the following conditions between $\rho_{1,1}$ and $\rho_{2,1}$:

$$\Delta \log \rho_{1,1} = \frac{\lambda_{12} n_2}{\pi} \left(\frac{A_2}{\rho_{2,1}} + \rho_{2,1} \right) \tag{112}$$

$$\Delta \log \rho_{2,1} = -\frac{\lambda_{12} n_1}{\pi} \left(\rho_{1,1} + \frac{A_1}{\rho_{1,1}} \right) . \tag{113}$$

The fact that $\rho_{1,1}$ and $\rho_{2,1}$ appear in a symmetric way in Eqs. (112) and (113), suggests the following ansatz:

$$\rho_{2,1} = \frac{A_3}{\rho_{1,1}} \tag{114}$$

with A_3 being a constant. It is easy to check that with this ansatz Eqs. (112) and (113) remain compatible provided:

$$\frac{A_2}{A_3} = \frac{n_1}{n_2} \quad \text{and} \quad \frac{A_3}{A_1} = \frac{n_1}{n_2} . \tag{115}$$

We choose A_1 to be the independent constant, while A_2 and A_3 are constrained by Eq. (115) to be dependent on A_1:

$$A_2 = \left(\frac{n_1}{n_2}\right)^2 A_1 \qquad A_3 = \frac{n_1}{n_2} A_1. \tag{116}$$

We are now left only with the task of computing the explicit expression of $\rho_{1,1}$. This may be obtained by solving the equation:

$$\Delta \log \rho_{1,1} = \frac{\lambda_{12} n_1}{\pi} \left(\frac{A_1}{\rho_{1,1}} + \rho_{1,1}\right) \tag{117}$$

The other quantities $\rho_{2,1}$, $\rho_{1,2}$ and $\rho_{2,2}$ can be derived using the relations (114), (100) and (101) respectively. Eq. (117) may be cast in a more familiar form by putting: $\eta = \ln\left(\frac{\rho_{1,1}}{\sqrt{A_1}}\right)$. After this substitution, Eq. (117) becomes the Euclidean cosh–Gordon equation with respect to η:

$$\Delta \eta = \frac{2\lambda_{12} n_1}{\pi} \sqrt{A_1} \cosh \eta \tag{118}$$

Next, it is possible to determine the magnetic fields $\boldsymbol{B}^{12}$ and $\boldsymbol{C}^{12}$ from Eqs. (106) and (107). In the Coulomb gauge, in fact, the two-dimensional vector potentials $\boldsymbol{B}^{12}$ and $\boldsymbol{C}^{12}$ can be represented using two scalar fields b^{12} and c^{12} as follows (see also Eq. (22)):

$$\boldsymbol{B}^{12} = (-\partial_2 b^{12}, \partial_1 b^{12}) \qquad \boldsymbol{C}^{12} = (-\partial_2 c^{12}, \partial_1 c^{12}) \tag{119}$$

Performing the above substitutions in Eqs. (106) and (107), it turns out that b^{12} and c^{12} satisfy the relations:

$$\Delta b^{12} = -\frac{n_1}{2\pi}(\rho_{1,1} + \frac{A_1}{\rho_{1,1}}) \tag{120}$$

$$\Delta c^{12} = -\frac{4 n_1 \pi \lambda_{12}}{\kappa}(\rho_{1,1} + \frac{A_1}{\rho_{1,1}}) \tag{121}$$

The solution of Eqs. (120) and (121) can be easily derived with the help of the method of the Green functions once the expression of $\rho_{1,1}$ is known. Finally, the phases $\omega_{1,1}$, $\omega_{1,2}$, $\omega_{2,1}$ and $\omega_{2,2}$ are computed using Eqs. (102)–(105). In fact, remembering that we assumed that $\omega_{1,1} = -\omega_{1,2}$ and $\omega_{2,1} = -\omega_{2,2}$ in (100) and (101) respectively, we have only to determine $\omega_{1,1}$ and $\omega_{2,1}$. By deriving Eq. (102) with respect to x^1 and Eq. (103) with respect to x^2, we obtain:

$$\begin{aligned} \lambda_{12} \partial_1 B_1^{12} &= \partial_1^2 \omega_{1,1} + \frac{1}{2} \partial_1 \partial_2 \log \rho_{1,1} \\ \lambda_{12} \partial_2 B_2^{12} &= \partial_2^2 \omega_{1,1} - \frac{1}{2} \partial_2 \partial_1 \log \rho_{1,1} \end{aligned} \tag{122}$$

On the other side, by adding term by term the above two equations and using the fact that in the Coulomb gauge the magnetic field $\boldsymbol{B}^{12}$ is completely transverse, it is possible to show that:

$$\Delta \omega_{1,1} = 0 \tag{123}$$

Proceeding in a similar way with Eq. (104) and (105) it is possible to derive also the relation satisfied by $\omega_{2,1}$:

$$\Delta \omega_{2,1} = 0 \tag{124}$$

7. Conclusions

In this work a $2s$-plat composed by N polymers forming a nontrivial link has been considered. In a $2s$-plats the number s of maxima and minima is fixed. With respect to the links of polymer rings discussed for instance in Ref. [52], that are not subjected to this constraint, the set of possible conformations of the links under investigation is limited. The differences that arise in the entropy and free energy of a $2s$-plat in comparison with general links are important both for biological and technological applications. Apart from the novelty of the subject, the representation as $2s$-plats of systems of knotted rings with non-trivial topological properties presents several advantages. One of them is the previously discussed possibility of using the bridge number, a topological invariant that improves the treatment of the topological constraints based only on the GLN of Refs. [56] and [52]. The more refined topological invariants that have been proposed up to now, for instance in [63] and [65], lead to field theoretical models that are far more complicated than the relatively simple model derived in this work. The feature of $2s$-plats that is more relevant for our purposes is that $2s$-plats may be decomposed into a set of $2s$ open and monotonic curves. Such curves can be interpreted as the conformations of $2s$ open polymer chains directed along an arbitrary direction. We have assumed here that this direction coincides with the z-axis. In Subsection 3.1 we have shown that this choice does not decrease the generality of our results.

The nontrivial interactions and the topological constraints make the energy density of the system complicated and nonlocal, but we have seen that it can be simplified with the introduction of auxiliary fields. The final model which we obtain is a standard field theory involving a set of complex scalar fields with sextic interactions at most. This model allows some phenomenological predictions that were a priori not obvious and that will be summarized below.

1. In the general case of a $2s$-plat the two-body interactions between the monomers, expressed in Eq. (29) by a potential $V(\boldsymbol{r}_2 - \boldsymbol{r}_1)$, can be screened or enhanced by the interactions in Eq. (35) that arise due to the presence of the topological constraints. This interference between non-topological and topological interactions is visible for example in Eq. (54). In fact, it is easy to realize that in the action $S_{part}(\vec{\Psi}^*_{a,I_a}, \vec{\Psi}_{a,I_a})$ the terms containing the third components of the BF-fields can be absorbed after a shift of the fields φ_{a,I_a}. This hints to a strong interplay between topological and non-topological interactions, since the former are mediated by the BF-fields, while the latter are propagated by the fields φ_{a,I_a}. Let us note that the effects of the forces of topological origin may result both in a reciprocal attraction or repulsion between the monomers. On the contrary, the short range two-body potential (31), which applies to the situation in which the polymers are immersed in a solution, can only be attractive if $V_0 < 0$ or repulsive if $V_0 > 0$.
2. The field theoretical model of polymeric $2s$-plats defined by Eqs. (63)–(68) shows that three-body forces become relevant in a system of N polymers linked together in which the topological constraints are imposed by means of the Gauss linking number. These three-body forces have been represented in the form of a Feynman diagram in Fig. 6-(c) and are described in Section 5. An example of process in which there are interactions between three monomers at once has been shown in Fig. 7. The existence of three-body interactions acting on the monomers was not predicted by previous calculations. This is probably because only the case $N = 2$ has been mainly treated so far. When $N = 2$, it turns out that the contribution of sextic interactions terms in the action of Eq. (65), which are responsible for the presence of the three-body forces, vanishes in the zero replica limit [55]. Besides, the appearance of three-body forces is not trivial and not easy to be predicted, because the Gauss linking num-

ber involves only interactions between pairs of monomers. Let us notice that the strengths of the two- and three-body forces are respectively proportional to λ_{ab} and λ_{ab}^2. The λ_{ab}'s are Fourier coefficients, so that they are not fixed, but can take any value from $-\infty$ to $+\infty$. This complicates the task of evaluating the strengths of these interactions in different regimes.

3. By using the splitting procedure presented in Section 2 and thanks to the introduction of auxiliary fields, the problem of the statistical mechanics of a $2s$-plat has been mapped into the dynamics of a system in which quasiparticles of different kinds are mixed together. In Ref. [42] it has been shown that systems of this type admit vortex solutions. Out of the self-duality regime, vortex magnetic lines associated with quasi-particles of different kind can repel or attract themselves. After a particular choice of the parameters of the theory, in which the coefficients g_{a,I_a}, $a = 1, 2$ and $I_a = 1, 2$ are all equal, a self-dual point is reached in which attractive and repulsive forces balance themselves and disappear. A similar phenomenon, but in a different model, has been recently found in Ref. [66]. In this work, the self-dual vortex conformations have been computed exactly and explicitly up to the solution of a cosh-Gordon equation.

The topological properties of the link formed by the $2s$-plat have been described here by using the Gauss linking invariant, which is related to the abelian BF-model of Eq. (34). When the BF-model is quantized in the Coulomb gauge, the topological constraints requiring that the Gauss linking numbers between pairs of rings are constant are apparently lost, being replaced by constraints on the winding numbers of the $2s$ open chains composing the plat. In Appendix C it has been shown in the case $s = 4$ that these constraints on the winding numbers of the chains are compatible with the original topological constraints on the Gauss linking numbers.

While abelian anyon field theories like those of Eq. (34) may be significant in quantum computing [67], it is rather nonabelian statistics that plays the main role in this kind of applications. Despite its limitations, our model is able to capture also part of the non-abelian features of the system. The reason is that the constraints on the Gauss linking numbers are applied together with the constraint on the $2s$-plat configuration, which cannot be destroyed because the $2s$ points of maxima and minima are kept fixed. As mentioned in the Introduction, if we start from an unlink consisting of a 4-plat, the system will never be able to attain the configuration of a Whitehead link and vice-versa, a 6-plat Whitehead link cannot turn into a 4-plat. By choosing $s = s_{min}$, where $2s_{min}$ is the least possible number of maxima and minima necessary to represent a given link, another topological invariant is added to our treatment besides the GLN, namely the bridge number. This combination of two invariants is much more powerful than the GLN alone. Of course, it should be kept in mind that it is impossible to constrain the topology of a knot or link with the help of a finite set of topological invariants. While the combined constraint provided by the GLN and the bridge number is much more powerful than the GLN alone, still the paths of the polymers are allowed to cross themselves during thermal fluctuations, implying that the freedom of changing topology remains. Moreover, in a forthcoming publication we will show how the present formalism can be applied to include in our approach not only the bridge number, but also much stronger constraints than the Gauss linking number. This possibility has been mentioned at the beginning of Section 3. This will pave the way to the treatment of polymer knots or links constructed from tangles. It is worthing to stress at this point that so far there is no satisfactory analytical model for the statistical mechanics of knots, at least comparable with that of links derived in [56]. The problem in the case of knots is that knot invariants are too complicated to be implemented in a field theory. For this reason, the derivation of a field theory describing the fluctuations of single knots in a solution, even with the restriction of fixing the $2s$ points of max-

ima and minima due to the plat configuration, would be an important progress in understanding the behavior of knotted polymer rings. Besides, these results could be relevant in biochemistry because nontrivial knot and link configurations appearing as a major pattern in DNA rings are mostly in the form of tangles [13].

Acknowledgements

F. Ferrari would like to thank E. Szuszkiewicz for pointing out Ref. [71] and inspiring the present work. He is also grateful to J. Wang for bringing to the attention the following papers that could be relevant for further developments toward the inclusion of non-abelian topological invariants: [68–70]. J. Paturej would like to acknowledge the support from the Polish Ministry of Science and Higher Education (Iuventus Plus: IP2015 059074). F. Ferrari and J. Paturej wish to thank heartily also M. Pyrka, V. G. Rostiashvili and T.A. Vilgis for fruitful discussions. The simulations reported in this work were performed in part using the HPC cluster HAL9000 of the Computing Centre of the Faculty of Mathematics and Physics at the University of Szczecin. This work results within the collaboration of the COST Action CA17139.

Appendix A. Parametrization of the paths Γ_{a,I_a}'s

In this Appendix we consider the set of directed paths Γ_{a,I_a}, $a = 1, \dots, N$ and $I_a = 1, \dots, 2s_a$ resulting after the decomposition of the loops $\Gamma_1, \dots, \Gamma_N$ in Section 2. In the general case, the set of points belonging to Γ_{a,I_a} can be described by the formula:

$$\Gamma_{a,I_a} = \left\{ \boldsymbol{r}_{a,I_a}(z_{a,I_a}) \;\middle|\; \begin{array}{c} a = 1, \dots, N; \qquad I_a = 1, \dots, 2s_a \\ \left\{ \begin{array}{ll} \tau_{a,I_a-1} \le z_{a,I_a} \le \tau_{a,I_a} & I_a \text{ odd} \\ \tau_{a,I_a} \le z_{a,I_a} \le \tau_{a,I_a-1} & I_a \text{ even} \end{array} \right. \end{array} \right\} \tag{125}$$

where the additional boundary conditions (4) and (5) are understood. They are necessary for granting the continuity of the loops Γ_a. For convenience, we report these conditions below:

$$\boldsymbol{r}_{a,I_a}(\tau_{a,I_a}) = \boldsymbol{r}_{a,I_a+1}(\tau_{a,I_a}) \qquad I_a = 1, \dots, 2s_a - 1 \tag{126}$$

$$\boldsymbol{r}_{a,1}(\tau_{a,0}) = \boldsymbol{r}_{a,2s_a}(\tau_{a,0}) \tag{127}$$

In Eq. (125) the two-dimensional vector $\boldsymbol{r}_{a,I_a}(z_{a,I_a})$ represents the projection of the trajectory Γ_{a,I_a} onto the plane x, y perpendicular to the z-axis. Let us note that we are using the same indexes I_a to label the trajectories Γ_{a,I_a} and the points τ_{a,I_a}. However, in the first case $I_a = 1, \dots, 2s_a$, while in the second case we have chosen $I_a = 0, \dots, 2s_a - 1$. The range of the indices I_a in the variables z_{a,I_a}'s and of the t_{a,I_a}'s that will be introduced later in this Appendix (see also Eq. (3) in Section 2) is the same as that of the indices labeling the trajectories Γ_{a,I_a}'s, i.e. $I_a = 1, \dots, 2s_a$.

The disadvantage of the variables z_{a,I_a}'s is that by definition they are always growing. In this way, the fact that the whole loop Γ_a is continuous and has a given orientation is not taken into account. Better variables, respecting both the continuity and orientation of the trajectories Γ_{a,I_a}, are the t_{a,I_a}'s, which are defined as follows:

$$t_{a,I_a} = z_{a,I_a} \qquad \text{when } I_a \text{ is odd} \tag{128}$$

$$t_{a,I_a} = -(z_{a,I_a} - \tau_{a,I_a}) + \tau_{a,I_a-1} \qquad \text{when } I_a \text{ is even.} \tag{129}$$

Assuming for instance that I_a is odd, then for any two consecutive trajectories Γ_{a,I_a} and Γ_{a,I_a+1} the range of the variables t_{a,I_a} and t_{a,I_a+1} is given by:

$$\tau_{a,I_a-1} \leq t_{a,I_a} \leq \tau_{a,I_a} \qquad I_a \text{ odd} \qquad 1 \leq I_a \leq 2s_a - 1 \tag{130}$$

Instead, if I_a is even:

$$\tau_{a,I_a-1} \geq t_{a,I_a} \geq \tau_{a,I_a} \qquad I_a \text{ even} \qquad 2 \leq I_a \leq 2s_a. \tag{131}$$

Let us recall that by our conventions the trajectories labeled by odd I_a's are oriented from a point of minimum to a point of maximum, while trajectories with even values of I_a go from a point of maximum to a point of minimum. Accordingly, the new variables t_{a,I_a} have been chosen in such a way that they increase from the minimum to the maximum when I_a is odd, while they decrease from the point of maximum to that of minimum when I_a is even. Finally, we provide the definition of the curves Γ_{a,I_a} parametrized with the help of the new variables t_{a,I_a}'s:

$$\Gamma_{a,I_a} = \left\{ \boldsymbol{r}_{a,I_a}(t_{a,I_a}) \;\middle|\; \begin{array}{c} a = 1, \dots, N; \qquad I_a = 1, \dots, 2s_a \\ \left\{ \begin{array}{ll} \tau_{a,I_a-1} \leq t_{a,I_a} \leq \tau_{a,I_a} & I_a \text{ odd} \\ \tau_{a,I_a-1} \geq t_{a,I_a} \geq \tau_{a,I_a} & I_a \text{ even} \end{array} \right. \end{array} \right\} \tag{132}$$

This is exactly Eq. (3). Of course, the boundary conditions (126) and (127), or equivalently (4) and (5), are always understood.

The variables t_{a,I_a} arise in a natural way when a curvilinear integral around the loop Γ_a is split into many trajectories Γ_{a,I_a}. In fact, let's consider for example integrals of the kind

$$I = \oint_{\Gamma_a} d\tilde{x}_a^\mu(d_a) A_\mu(\tilde{x}_a(d_a)) \tag{133}$$

where the symbol $\tilde{x}_a^\mu(d_a) = (\tilde{\boldsymbol{r}}_a(d_a), \tilde{x}_a^3(d_a))$ denotes the points of the trajectory Γ_a parametrized in terms of the arc-length d_a, $0 \leq d_a \leq L_a$. $A_\mu(\tilde{x}_a(d_a))$ is an abelian gauge field on $\mathbb{R}^3$. It is easy to show that, after splitting the loop Γ_a into the trajectories Γ_{a,I_a}, on each of these trajectories it is possible to change the arc-length d_a with the parameters t_{a,I_a}. If one does that, the curvilinear integral I of Eq. (133) becomes parametrized by the variables t_{a,I_a} and may be expressed as follows

$$I = \sum_{I_a=1}^{2s_a} \int_{\tau_{a,I_a-1}}^{\tau_{a,I_a}} \left[\frac{d\boldsymbol{r}_{a,I_a}(t_{a,I_a})}{dt_{a,I_a}} \cdot \boldsymbol{A}(\boldsymbol{r}_{a,I_a}(t_{a,I_a}), t_{a,I_a}) + A_3(\boldsymbol{r}_{a,I_a}(t_{a,I_a}), t_{a,I_a}) \right] \tag{134}$$

where

$$t_{a,I_a} = \tilde{x}_a^3(d_a) \qquad \boldsymbol{r}_{a,I_a}(t_{a,I_a}) = \boldsymbol{r}_{a,I_a}(\tilde{x}_a^3(d_a)) = \tilde{\boldsymbol{r}}_a(d_a). \tag{135}$$

Of course, the above equation is valid only if d_a is restricted on the trajectory Γ_{a,I_a}, i.e., $\delta_{a,I_a-1} \leq d_a \leq \delta_{a,I_a}$. The δ_{a,I_a}'s denote the values of the arc-length at the points of maxima and minima of the $2s_a$-plat Γ_a. Clearly, $\tilde{x}_a^3(\delta_{a,I_a}) = \tau_{a,I_a}$.

Appendix B. The length L of a directed polymer as a function of the height

In this Appendix we consider the partition function

$$\mathcal{Z} = \int \mathcal{D}\boldsymbol{r}(z) e^{-S} \tag{136}$$

where S is the action of the free open polymer, whose path Γ is parametrized by means of the height z defined in some interval $[\tau_0, \tau_1]$:

$$S = g \int_{\tau_0}^{\tau_1} dz \left| \frac{d\boldsymbol{r}}{dz} \right|^2 \tag{137}$$

We want now to determine how the total length of the curve Γ depends on the constant parameter g. To understand what we mean by that, let us consider the standard case of an ideal chain whose path is parametrized with the help of the arc-length σ. We denote with a the average statistical length (Kuhn length) of the N segments composing the polymer. In the limit of large N and small a such that the product Na is constant, the total length L of the polymer satisfies the relation

$$L = Na \tag{138}$$

We wish to obtain a similar identity connecting L with N and g in the present situation, which is somewhat different. To this purpose, we first dicretize the interval of integration $[\tau_0, \tau_1]$ splitting it into N small segments of length:

$$\Delta z = \frac{\tau_1 - \tau_0}{N} \tag{139}$$

As a consequence, we may approximate the action as follows:

$$S \sim g \sum_{w=1}^{N} \left| \frac{\Delta \boldsymbol{r}_w}{\Delta z} \right|^2 \Delta z \tag{140}$$

where the symbol $\Delta \boldsymbol{r}_w$ means

$$\Delta \boldsymbol{r}_w = \boldsymbol{r}_{w+1} - \boldsymbol{r}_w \tag{141}$$

and

$$\boldsymbol{r}_w = \boldsymbol{r}(\tau_0 + w\Delta z) \tag{142}$$

The discretized partition function becomes thus the partition function of a random chain composed by N segments:

$$\mathcal{Z}_{disc} = \int \prod_{w=1}^{N} d\boldsymbol{r}_w e^{-\sum_{w=1}^{N} g \frac{|\Delta \boldsymbol{r}_w|^2}{\Delta z}} \tag{143}$$

Using simple trigonometric arguments it is easy to realize that the length of each segment is:

$$\Delta L = \sqrt{|\Delta \boldsymbol{r}_w|^2 + (\Delta z)^2} \tag{144}$$

This is of course an average length, dictated by the fact that, from Eq. (143), the values of $|\Delta \boldsymbol{r}_w|$ should be gaussianly distributed around the point:

$$|\Delta \boldsymbol{r}_w|^2 = \frac{\Delta z}{g} \tag{145}$$

In the limit $\Delta z \to 0$, the distribution of length of $\Delta \boldsymbol{r}_w$ becomes the Dirac δ-function:

$$\lim_{\Delta z \to 0} \frac{1}{2} \sqrt{\frac{g}{\Delta z}} e^{-g|\Delta \boldsymbol{r}_w|^2/\Delta z} \sim \delta\left(|\Delta \boldsymbol{r}_w| - \sqrt{\frac{\Delta z}{g}} \right) \tag{146}$$

If N is large enough, we can therefore conclude that the total length of the chain Γ is:

$$L \sim N\Delta L = N\sqrt{\frac{\Delta z}{g} + (\Delta z)^2} \tag{147}$$

Since $N\Delta z = \tau_1 - \tau_0$, we get:

$$L^2 = |\tau_1 - \tau_0|^2 + \frac{N(\tau_1 - \tau_0)}{g} \tag{148}$$

In the limit $N \to \infty$, while keeping the ratio $\frac{N}{g}$ finite, Eq. (148) becomes the desired relation between the length of Γ and g which replaces Eq. (138).

Appendix C. The expression of the Gauss linking invariant in the Coulomb gauge

To fix the ideas, we will study here the particular case of a 4-plat. In the partition function (33) we isolate only the terms in which the BF fields appear, because the other contributions are not connected to topological constraints and thus are not relevant. As a consequence, we have just to compute the following partition function:

$$\mathcal{Z}_{BF,CG}(\lambda) = \int \mathcal{D}B_\mu \mathcal{D}C_\mu e^{-iS_{BF,CG} - S_{top}} \tag{149}$$

where the BF action in the Coulomb gauge $S_{BF,CG}$ has been already defined in Eq. (21) and S_{top} has been given in Eq. (35). In the case of a 4-plat, S_{top} becomes:

$$\begin{aligned} S_{top} = i\lambda \int_{\tau_{1,0}}^{\tau_{1,1}} dt \left[\frac{dx^\mu_{1,1}(t)}{dt} B_\mu(\boldsymbol{r}_{1,1}(t), t) - \frac{dx^\mu_{1,2}(t)}{dt} B_\mu(\boldsymbol{r}_{1,2}(t), t) \right] \\ + \frac{i\kappa}{8\pi^2} \int_{\tau_{2,0}}^{\tau_{2,1}} dt \left[\frac{dx^\mu_{2,1}(t)}{dt} C_\mu(\boldsymbol{r}_{2,1}(t), t) - \frac{dx^\mu_{2,2}(t)}{dt} C_\mu(\boldsymbol{r}_{2,2}(t), t) \right] \end{aligned} \tag{150}$$

where we recall that $x^\mu_{a,I}(t) = (\boldsymbol{r}_{a,I}(t), t)$, $a = 1, 2$, $I = 1, 2$. For simplicity of the notation, in this Appendix we use λ instead of λ_{12}. Using the Chern-Simons propagator of Eqs. (25)-(26), it is easy to evaluate the path integral over the gauge fields in Eq. (149). The result, after two simple Gaussian integrations, is:

$$Z_{BF,CG}(\lambda) = \exp\left\{ \frac{i\lambda}{2\pi} \sum_{I,J=1}^{2} (-1)^{I+J-2} \epsilon_{ij} \int_{\tau_0}^{\tau_1} d(x^i_{1,I}(t) - x^i_{2,J}(t)) \frac{(x^j_{1,I}(t) - x^j_{2,J}(t))}{\left|\boldsymbol{r}_{1,I}(t) - \boldsymbol{r}_{2,J}(t)\right|^2} \right\} \tag{151}$$

In the above equation we have put for simplicity:

$$\begin{aligned} \tau_0 &= \max[\tau_{1,0}, \tau_{2,0}] \\ \tau_1 &= \min[\tau_{1,1}, \tau_{2,1}] \end{aligned} \tag{152}$$

For instance, if the polymer configurations are as in Fig. 8, we have that $\tau_0 = \tau_{1,0}$ and $\tau_1 = \tau_{2,1}$. Moreover, we remember that in our notation $\boldsymbol{r}_{a,I}(t) = (x^1_{a,I}(t), x^2_{a,I}(t))$. Apparently, the

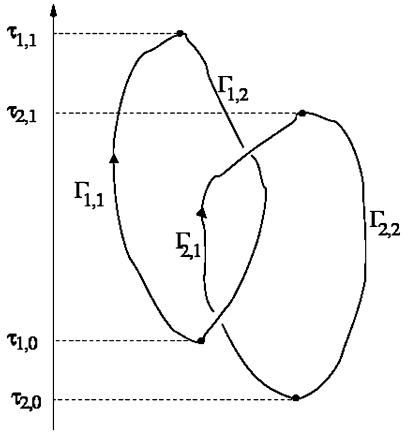

Fig. 8. Example of configuration of a 4-plat.

elements of the loops Γ_1 and Γ_2 which lie below τ_0 and above τ_1 do not take the part in the topological interactions. Thus is due to the presence of the Dirac δ-function $\delta(t-t')$ in the components of the Chern-Simons propagator (25)-(26). However, we will see later that also the contributions of these missing parts are present in the expression of $Z_{BF,CG}(\lambda)$. In order to proceed, we notice that the exponent of the right hand side of Eq. (151) consists in a sum of integrals over the time t of the kind:

$$D_{1,I;2,J}(\tau_1) - D_{1,I;2,J}(\tau_0) = \epsilon_{ij} \int_{\tau_0}^{\tau_1} d\left(x^i_{1,I}(t) - x^i_{2,J}(t)\right) \frac{(x^j_{1,I}(t) - x^j_{2,J}(t))}{\left|\boldsymbol{r}_{1,I}(t) - \boldsymbol{r}_{2,J}(t)\right|^2} \tag{153}$$

The above integrals can be computed exactly. It is in fact well known that the function $D_{1,I;2,J}(t)$ is the winding angle of the vector $\boldsymbol{r}_{1,I}(t) - \boldsymbol{r}_{2,J}(t)$ at time t:

$$D_{1,I;2,J}(t) = \arctan\left(\frac{x^1_{1,I}(t) - x^1_{2,J}(t)}{x^2_{1,I}(t) - x^2_{2,J}(t)}\right) \tag{154}$$

Thus, the quantity $D_{1,I;2,J}(\tau_1) - D_{1,I;2,J}(\tau_0)$ is a difference of winding angles which measures how many times the trajectory $\Gamma_{1,I}$ turns around the trajectory $\Gamma_{2,J}$ in the slice of time $\tau_0 \leq t \leq \tau_1$. At this point, without any loss of generality, we suppose that the configurations of the curves Γ_1 and Γ_2 are such that the maxima and minima $\tau_{a,I}$ are ordered as follows:

$$\tau_{2,0} < \tau_{1,0} < \tau_{2,1} < \tau_{1,1} \tag{155}$$

As example of loop configurations that respect this ordering is given in Fig. 8. As a consequence, we have:

$$\tau_0 = \tau_{1,0} \qquad \text{and} \qquad \tau_1 = \tau_{2,1} \tag{156}$$

Now we notice that the logarithm of the gauge partition function $\mathcal{Z}_{BF,CG}(\lambda)$ in Eq. (151) contains a sum of differences of the winding angles defined in Eq. (154):

$$\frac{2\pi \log \mathcal{Z}_{BF,CG}(\lambda)}{i\lambda} = \big[D_{1,1;2,1}(\tau_{2,1}) - D_{1,1;2,1}(\tau_{1,0}) + D_{1,2;2,2}(\tau_{2,1}) - D_{1,1;2,2}(\tau_{2,1}) + D_{1,2;2,1}(\tau_{1,0}) - D_{1,2;2,1}(\tau_{2,1}) + D_{1,1;2,2}(\tau_{1,0}) - D_{1,2;2,2}(\tau_{1,0})\big] \tag{157}$$

Further, assuming that the curves Γ_1 and Γ_2 are oriented as in Fig. 8. If we start from the minimum point at $\tau_0 = \tau_{1,0}$, we can isolate in the right hand side of Eq. (157) the following four contributions:

1. In the time slice $\tau_{1,0} \leq t \leq \tau_{2,1}$ the angle which measures the winding of the trajectory $\Gamma_{1,1}$ around the trajectory $\Gamma_{2,1}$ is given by the difference $D_{1,1;2,1}(\tau_{2,1}) - D_{1,1;2,1}(\tau_{1,0})$.
2. In the region $\tau_{2,1} \leq t \leq \tau_{1,1}$ only the loop Γ_1 continues to evolve, going first upwards with the trajectory $\Gamma_{1,1}$ and then downwards with $\Gamma_{1,2}$. After this evolution, the winding angle between the two loops Γ_1 and Γ_2 has changed by the quantity $D_{1,2;2,2}(\tau_{2,1}) - D_{1,1;2,2}(\tau_{2,1})$.
3. Next, in the region $\tau_{2,1} \geq t \geq \tau_{1,0}$, the winding angle which measures how many times the trajectory $\Gamma_{1,2}$ winds up around $\Gamma_{2,2}$ is given by the difference $D_{1,2;2,1}(\tau_{1,0}) - D_{1,2;2,1}(\tau_{2,1})$.
4. Finally, in the region $\tau_{1,0} \geq t \geq \tau_{2,0}$ only the second loop Γ_2 continues to evolve, going first downwards with the curve $\Gamma_{2,2}$ and then upwards with $\Gamma_{2,1}$. The net effect of this evolution is that the winding angle between Γ_1 and Γ_2 changes by the quantity $D_{1,1;2,2}(\tau_{1,0}) - D_{1,2;2,2}(\tau_{1,0})$.

It is thus clear that the right hand side of Eq. (157), apart from a proportionality factor $i\lambda$, counts how many times the loop Γ_1 winds around the second loop Γ_2. If we wish to identify the quantity in the right hand side of Eq. (157) with the Gauss linking number $\chi(\Gamma_1, \Gamma_2)$, we should check for consistency that it takes only integer values as the Gauss linking number does. Indeed, it is easy to see that, modulo 2π, the following identities are holding:

$$\begin{aligned} D_{1,1;2,1}(\tau_{2,1}) &= D_{1,1;2,2}(\tau_{2,1}) \\ D_{1,1;2,2}(\tau_{1,0}) &= D_{1,2;2,2}(\tau_{1,0}) \\ D_{1,2;2,2}(\tau_{2,1}) &= D_{1,2;2,1}(\tau_{2,1}) \\ D_{1,1;2,1}(\tau_{1,0}) &= D_{1,2;2,1}(\tau_{1,0}) \end{aligned} \tag{158}$$

For example, the first of the above equalities states that the angle formed by the vector $\boldsymbol{r}_{1,1} - \boldsymbol{r}_{2,1}$ connecting the trajectories $\Gamma_{1,1}$ and $\Gamma_{2,1}$ at the height $\tau_{2,1}$ is equal to the angle formed by the vector $\boldsymbol{r}_{1,1} - \boldsymbol{r}_{2,2}$ connecting the trajectories $\Gamma_{1,1}$ and $\Gamma_{2,2}$ at the same height. The reason of this identity is trivial: At that height, the trajectories $\Gamma_{2,1}$ and $\Gamma_{2,2}$ are connected together at the same point. Applying the above relations to Eq. (157), one may prove that:

$$\frac{2\pi \log \mathcal{Z}_{BF,CG}(\lambda)}{i\lambda} = 0 \qquad \text{mod } 2\pi \tag{159}$$

As a consequence, we can write:

$$\mathcal{Z}_{BF,CG}(\lambda) = e^{i\lambda\chi(\Gamma_1,\Gamma_2)} \tag{160}$$

where $\chi(\Gamma_1, \Gamma_2)$ is the Gauss linking number. Concluding, the above analysis shows that also in the Coulomb gauge the BF fields in the polymer partition function (33) fix the topological constraints (7) correctly, in full consistency with the results obtained in the covariant gauges. Of course this consistency was expected due to gauge invariance. Yet, it is interesting that, using the Coulomb gauge, one may express the Gauss linking number invariant in a way that is quite different from the usual form given in Eq. (6).

References

[1] S.F. Edwards, Proc. Phys. Soc. 91 (1967) 513;
Proc. Phys. Soc. 92 (1967) 9.
[2] R.D. Kamien, P. Le Doussal, D. Nelson, Phys. Rev. A 45 (1992) 8727.
[3] A.Yu. Grosberg, Phys. Usp. 40 (1997) 12.
[4] W.R. Taylor, Nature (London) 406 (2000) 916.
[5] V. Katritch, J. Bednar, D. Michoud, R.G. Scharein, J. Dubochet, A. Stasiak, Nature 384 (1996) 142.
[6] V. Katritch, W.K. Olson, P. Pieranski, J. Dubochet, A. Stasiak, Nature 388 (1997) 148.
[7] M.A. Krasnow, A. Stasiak, S.J. Spengler, F. Dean, T. Koller, N.R. Cozzarelli, Nature 304 (1983) 559.
[8] B. Laurie, V. Katritch, J. Dubochet, A. Stasiak, Biophys. J. 74 (1998) 2815.
[9] J.I. Sułkowksa, P. Sułkowksa, P. Szymczak, M. Cieplak, Phys. Rev. Lett. 100 (2008) 058106.
[10] J.F. Marko, Phys. Rev. E 79 (2009) 051905.
[11] Z. Liu, E.L. Zechiedrich, H.S. Chan, Biophys. J. 90 (2006) 2344.
[12] S.A. Wasserman, N.R. Cozzarelli, Science 232 (1986) 951.
[13] D.W. Sumners, Knot theory and DNA, in: D.W. Sumners (Ed.), New Scientific Applications of Geometry and Topology, in: Proceedings of Symposia in Applied Mathematics, vol. 45, American Mathematical Society, Providence, RI, 1992, p. 39.
[14] A.V. Vologodski, A.V. Lukashin, M.D. Frank-Kamenetski, V.V. Anshelevich, Zh. Eksp. Teor. Fiz. 66 (1974) 2153;
Sov. Phys. JETP 39 (1975) 1059;
M.D. Frank-Kamenetskii, A.V. Lukashin, A.V. Vologodskii, Nature (London) 258 (1975) 398.
[15] E. Orlandini, S.G. Whittington, Rev. Mod. Phys. 79 (2007) 611;
C. Micheletti, D. Marenduzzo, E. Orlandini, Phys. Rep. 504 (2011) 1.
[16] S.D. Levene, C. Donahue, T.C. Boles, N.R. Cozzarelli, Biophys. J. 69 (1995) 1036.
[17] T. Vettorel, A.Yu. Grosberg, K. Kremer, Phys. Biol. 6 (2009) 025013.
[18] P. Virnau, Y. Kantor, M. Kardar, J. Am. Chem. Soc. 127 (43) (2005) 15102.
[19] P. Pierański, S. Przybył, A. Stasiak, Eur. Phys. J. E, Soft Matter 6 (2) (2001) 123.
[20] J. Yan, M.O. Magnasco, J.F. Marko, Nature 401 (1999) 932.
[21] J. Arsuaga, M. Vazquez, S. Trigueros, D.W. Sumners, J. Roca, Proc. Natl. Acad. Sci. USA 99 (2002) 5373.
[22] J. Arsuaga, M. Vazquez, P. McGuirk, S. Trigueros, D.W. Sumners, J. Roca, Proc. Natl. Acad. Sci. USA 102 (2005) 9165.
[23] F. Ferrari, J. Paturej, M. Piątek, T.A. Vilgis, J. Math. Phys. 52 (2011) 043301.
[24] R. Potestio, C. Micheletti, H. Orland, PLoS Comput. Biol. 6 (7) (2010) e1000864.
[25] C. Cardelli, L. Tubiana, V. Bianco, F. Nerattini, C. Dellago, I. Coluzza, Macromolecules 51 (21) (2018) 8346.
[26] E. Orlandini, A.L. Stella, C. Vanderzande, F. Zonta, J. Phys. A, Math. Theor. 41 (12) (2008) 122002.
[27] R. Metzler, A. Hanke, P.G. Dommersnes, Y. Kantor, M. Kardar, Phys. Rev. Lett. 88 (2002) 188101.
[28] P. Pieranski, S. Clausen, G. Helgesen, A.T. Skjeltorp, Phys. Rev. Lett. 77 (1996) 1620.
[29] Y. Diao, C. Ernst, E.J. Janse van Rensburg, in: A. Stasiak, V. Katritch, L.H. Kauffman (Eds.), Ideal Knots, World Scientific, Singapore, 1998, p. 52.
[30] D.W. Sumners, Not. Am. Math. Soc. 42 (5) (1995) 528.
[31] L. Faddeev, A.J. Niemi, Nature 387 (1997) 58.
[32] N.P. King, et al., Proc. Natl. Acad. Sci. USA 107 (2010) 20732.
[33] H. Kleinert, Path Integrals in Quantum Mechanics, Statistics, Polymer Physics, and Financial Markets, 3rd ed., World Scientific Publishing, Singapore, 2003.
[34] J.S. Birman, Braids, Links, and Mapping Class Groups, Princeton University Press, 1974.
[35] M. Heusener, Topol. Appl. 127 (2003) 175.
[36] L.H. Kauffman, Int. J. Mod. Phys. B 6 (11&12) (1992) 1765.
[37] L. Crane, Commun. Math. Phys. 135 (1991) 615.
[38] J. Alexander, Proc. Natl. Acad. Sci. USA 9 (1963) 103–124.
[39] Y. Moriah, Heegaard splittings of knot exteriors, Geom. Topol. Monogr. 12 (2007) 191–232.
[40] C.C. Adams, The Knot Book, American Mathematical Society, Providence, Rhode Island, 2004.
[41] I.K. Darch, R.G. Scharein, Bioinformatics 22 (14) (2006) 1790.
[42] F. Ferrari, Phys. Lett. A 323 (2004) 351, arXiv:cond-mat/0401104.
[43] S. Das Sarma, M. Freedman, C. Nayak, Topological quantum computation, Phys. Today 59 (7) (2006) 32.
[44] C. Nayak, S.H. Simon, A. Stern, M. Freedman, S. Das Sarma, Rev. Mod. Phys. 80 (2008) 1083.
[45] F. Wilczek, New kinds of quantum statistics, in: The Spin, in: Progress in Mathematical Physics, vol. 55, 2009, p. 61.

[46] V. Goldman, J. Liu, A. Zaslavsky, Phys. Rev. B 71 (2005) 153303;
F. Camino, F. Zhou, V. Goldman, Phys. Rev. Lett. 98 (2007) 076805.
[47] G. Ben-Shach, C.R. Laumann, I. Neder, A. Yacoby, B.I. Halperin, Phys. Rev. Lett. 110 (2013) 106805.
[48] V. Gurarie, L. Radzihovsky, A.V. Andreev, Phys. Rev. Lett. 94 (2005) 230403.
[49] M. Dolev, M. Heiblum, V. Umansky, A. Stern, D. Mahalu, Nature 452 (2008) 829;
I. Radu, J. Miller, C. Marcus, M. Kastner, L. Pfeiffer, K. West, Science 320 (2008) 899.
[50] B. Field, T. Simula, Quantum Sci. Technol. 3 (4) (2018) 045004.
[51] J. Froehlich, C. King, Commun. Math. Phys. 126 (1) (1989) 167.
[52] F. Ferrari, H. Kleinert, I. Lazzizzera, Field theory of N entangled polymers, Int. J. Mod. Phys. B 14 (32) (2000) 3881, arXiv:cond-mat/0005300.
[53] F. Ferrari, Ann. Phys. (Leipz.) 11 (4) (2002) 255.
[54] See e.g., G. Decher, E. Kuchinka, H. Ringsdorf, J. Venzmer, D. Bitter-Suermann, C. Weisgerber, Angew. Makromol. Chem. 71 (1989) 166;
J. Simon, M. Kühner, H. Ringsdorf, E. Sackmann, Chem. Phys. Lipids 76 (2) (1995) 241;
G. Blume, G. Cevc, Biochim. Biophys. Acta 1029 (1990) 91;
D.D. Lasic, F.J. Martin, A. Gabizon, S.K. Huang, D. Papahadjopoulos, Biochim. Biophys. Acta 1070 (1991) 187.
[55] F. Ferrari, I. Lazzizzera, Nucl. Phys. B 559 (3) (1999) 673.
[56] F. Ferrari, I. Lazzizzera, Phys. Lett. B 444 (1998) 167.
[57] J.M.F. Labastida, Chern-Simons gauge theory: ten years after, AIP Conf. Proc. 484 (1999) 1.
[58] F. Ferrari, I. Lazzizzera, Perturbative analysis of the Chern–Simons field theory in the Coulomb gauge, Int. J. Mod. Phys. A 13 (1998) 1773, arXiv:hep-th/9611224.
[59] F. Ferrari, I. Lazzizzera, J. Phys. A, Math. Gen. 32 (1999) 1347, arXiv:hep-th/9803008.
[60] M. Blau, G. Thompson, Ann. Phys. 205 (1991) 130;
M. Blau, G. Thompson, Ann. Phys. 205 (1991) 130;
D. Birmingham, M. Blau, M. Rakowski, G. Thompson, Phys. Rep. 209 (1991) 129.
[61] M. Kardar, J. Appl. Phys. 61 (1987) 3601;
M. Kardar, G. Parisi, Y.-C. Zhang, Phys. Rev. Lett. 56 (1986) 889;
M. Kardar, Y.-C. Zhang, Phys. Rev. Lett. 58 (1987) 2087.
[62] P.G. de Gennes, Phys. Lett. A 38 (1972) 339;
J. des Cloiseaux, Phys. Rev. A 10 (1974) 1665;
V.J. Emery, Phys. Rev. B 11 (1975) 239.
[63] F. Ferrari, Topological field theories with non-semisimple gauge group of symmetry and engineering of topological invariants, in: O. Kovras (Ed.), Trends in Field Theory Research, ISBN 1-59454-123-X, Nova Science Publishers, 2005. See also the reprint of this article in: O. Kovras (Ed.), Current Topics in Quantum Field Theory Research, Nova Science Publishers, 2006, ISBN: 1-60021-283-2.
[64] F. Wilczek, Phys. Rev. Lett. 69 (1992) 132.
[65] F. Ferrari, M.R. Piątek, Y. Zhao, A topological field theory for Milnor's triple linking number, J. Phys. A, Math. Theor. 48 (2015) 275402, arXiv:1411.6429.
[66] M.C. Diamantini, C.A. Trugenberger, Higgsless superconductivity from topological defects in compact BF terms, arXiv:1408.5066.
[67] D.F. Milne, N.V. Korolkova, P. van Loock, Phys. Rev. A 85 (5) (2012) 052325.
[68] J. Wang, Z.-C. Gu, X.-G. Wen, Phys. Rev. Lett. 114 (2015) 031601.
[69] P. Putrov, J. Wang, S.-T. Yau, Ann. Phys. 384C (2017) 254.
[70] J. Wang, X.-G. Wen, E. Witten, Phys. Rev. X 8 (2018) 031048.
[71] G.P. Collins, Sci. Am. 294 (4) (2006) 56.